

Photovoltaic Manufacturing Cost and Throughput Improvements for Thin-Film CIGS-Based Modules

**Phase I Technical Report
July 1998 — July 1999**

S. Wiedeman and R.G. Wendt
*Global Solar Energy, L.L.C.
Tucson, Arizona*



NREL

National Renewable Energy Laboratory

1617 Cole Boulevard
Golden, Colorado 80401-3393

NREL is a U.S. Department of Energy Laboratory
Operated by Midwest Research Institute • Battelle • Bechtel

Contract No. DE-AC36-99-GO10337

Photovoltaic Manufacturing Cost and Throughput Improvements for Thin-Film CIGS-Based Modules

**Phase I Technical Report
July 1998 — July 1999**

S. Wiedeman and R.G. Wendt
*Global Solar Energy, L.L.C.
Tucson, Arizona*

NREL Technical Monitor: R.L. Mitchell

Prepared under Subcontract No. ZAX-8-17647-11



NREL

National Renewable Energy Laboratory

1617 Cole Boulevard
Golden, Colorado 80401-3393

NREL is a U.S. Department of Energy Laboratory
Operated by Midwest Research Institute • Battelle • Bechtel

Contract No. DE-AC36-99-GO10337

NOTICE

This report was prepared as an account of work sponsored by an agency of the United States government. Neither the United States government nor any agency thereof, nor any of their employees, makes any warranty, express or implied, or assumes any legal liability or responsibility for the accuracy, completeness, or usefulness of any information, apparatus, product, or process disclosed, or represents that its use would not infringe privately owned rights. Reference herein to any specific commercial product, process, or service by trade name, trademark, manufacturer, or otherwise does not necessarily constitute or imply its endorsement, recommendation, or favoring by the United States government or any agency thereof. The views and opinions of authors expressed herein do not necessarily state or reflect those of the United States government or any agency thereof.

Available electronically at <http://www.doe.gov/bridge>

Available for a processing fee to U.S. Department of Energy
and its contractors, in paper, from:

U.S. Department of Energy
Office of Scientific and Technical Information
P.O. Box 62
Oak Ridge, TN 37831-0062
phone: 865.576.8401
fax: 865.576.5728
email: reports@adonis.osti.gov

Available for sale to the public, in paper, from:

U.S. Department of Commerce
National Technical Information Service
5285 Port Royal Road
Springfield, VA 22161
phone: 800.553.6847
fax: 703.605.6900
email: orders@ntis.fedworld.gov
online ordering: <http://www.ntis.gov/ordering.htm>



Executive Summary

Interest in thin film photovoltaics (PV) has expanded dramatically in the last five years, but commercial use remains limited by performance, cost and reliability. Of all the thin film systems, copper indium gallium diselenide (CIGS) has demonstrated the greatest potential for achieving high performance at a low cost. The highest quality CIGS has been formed by multi-source co-evaporation, a technique pioneered in this country by researchers at NREL. Multi-source co-evaporation is also potentially the fastest and most cost-effective method of CIGS absorber deposition.

Global Solar Energy (GSE) has adapted multi-source co-evaporation of CIGS to large area, roll-to-roll processing on flexible substrates, enabling many advantages in manufacturing and product capabilities. Roll-to-roll processing enables a low cost, automated continuous manufacturing process. Flexible substrates enable product application in unique as well as traditional areas.

The primary objectives of the GSE Photovoltaic Manufacturing Technology (PV-MAT) subcontract are directed toward reducing cost and expanding the production rate of thin film CIGS based PV modules on flexible substrates. Improvements will be implemented in monolithic integration, CIGS deposition, contact deposition and in-situ CIGS control and monitoring. Specific goals of the three-year contract are:

- **Monolithic Integration**
 - Increase integration speed by developing high speed, all-laser scribing processes that are more than 100% faster than the baseline process and offer clean, selective scribing.
 - Increase capacity and substantially reduce module area losses by replacing conventional screen-printing with industrial, high-speed ink-jet printing to dispense insulating materials with high accuracy into laser scribes.
- **Absorber Deposition**
 - Increase absorber layer deposition rate by 75% in the large area, continuous GSE process, increasing throughput and reducing labor and capital costs.
 - Integrate a parallel detector spectroscopic ellipsometer (PDSE) with mathematical algorithms for *in-situ* control of CIGS absorber enabling runs of over 300 meters of moving substrate while ensuring uniform properties.
 - Enhance health and safety by reducing selenium waste generation through modifications to the reactor and Se delivery method.
- **Back Contact Deposition**
 - Reduce back contact cost and increase operation yield by using improved back contact materials.

In Phase 1 of this effort, GSE has attacked many of the highest risk aspects of each task with success. All-laser, selective scribing processes for CIGS have been developed, and many end-of-contract goals for scribing speed have been exceeded in the first year. High-speed ink-jet

deposition of insulating material in the scribes now appears to be a viable technique, again exceeding some end-of-contract goals in the first year.

Absorber deposition of CIGS was reduced corresponding to throughput speeds of up to 24-in./min., also exceeding an end of contract goal. Alternate back contact materials have been identified that show potential as candidates for replacement of higher cost molybdenum, and a novel, real time monitoring technique (PDSE) has shown remarkable sensitivity to relevant properties of the CIGS absorber layer for use as a diagnostic tool.

Table of Contents

	<u>Page</u>
-- Executive Summary.....	i
-- List of Figures.....	v
-- List of Tables.....	vii
-- References	vii
1.0 Task 1 – High Speed, All Laser Scribing Processes	1
1.1 Introduction.....	1
1.2 Task Objectives	1
1.3 Technical Approach.....	2
1.4 Results.....	2
1.4.1 Equipment Status	2
1.4.2 Scribe Interconnect Development.....	4
1.4.2.1 Back Contact Scribe	4
1.4.2.2 Front Contact Scribe	5
1.4.2.3 Interconnect (or “via”) Scribe.....	6
1.5 Conclusions and Future Work	7
2.0 Task 2 – Ink-Jet Technology for Insulator Deposition in Scribes	
2.1 Introduction	8
2.2 Task Objectives	8
2.3 Technical Approach	9
2.4 Results	9
2.4.1 Linewidth Improvement	10
2.4.2 Process Speed, Compatibility	11
2.5 Conclusions and Future Work	12
3.0 Task 3 – High Rate CIGS Deposition	
3.1 Introduction	13
3.2 Task Objectives	13
3.3 Technical Approach.....	14
3.4 Results	15
3.4.1 Source Design	15
3.4.2 Materials Flux Uniformity	15
3.4.3 CIGS Material Quality Using a Low Temperature Process	17
3.4.4 High Rate CIGS Deposition	18
3.4.5 Impurity Incorporation in the CIGS	21
3.5 Conclusions and Future Work	23
4.0 Task 4 – In-Situ Sensors for Process Control of Roll-to-Roll CIGS	
4.1 Introduction	24
4.2 Task Objectives	25
4.3 Technical Approach.....	25
4.4 Results	27
4.5 Conclusions and Future Work	30

5.0 Task 5 - Alternative Back Contacts

5.1 Introduction	32
5.2 Task Objectives	32
5.3 Technical Approach.....	33
5.4 Results	33
5.4.1 Background and Candidate Material Identification	33
5.4.2 Single Layer Back Contacts	35
5.4.2.1 Thermodynamic Analysis.....	35
5.4.2.2 Back Contact Deposition	35
5.4.2.3 CIGS Deposition.....	36
5.4.2.4 Large Area Deposition	39
5.4.3 Bi-layer Alternate Back Contact.....	39
5.4.3.1 Bi-layer Back Contact Deposition.....	39
5.4.3.2 CIGS Deposition on Bi-layer Back Contacts	40
5.5 Conclusions and Future Work	41

List of Figures

<u>Figure</u>	<u>Page</u>
1.1A	Example scribe on CIGS/Mo/polyimide made using one method of beam delivery, for comparison to figure 1B.....3
1.1B	A scribe on the same material shown in figure 1A using a different means of beam delivery. Note the asymmetry and damage.....3
1.2	Sequence of operations to form an interconnected module on flexible substrate4
1.3	Resultant module interconnect structure on flexible substrate.4
1.4A	Micrograph of a back contact scribe made through CdS/CIGS/Mo on polyimide. (L902804a.jpg)5
1.4B	Perspective view of a back contact scribe through CdS/CIGS/Mo on polyimide. (L902804b.jpg).....5
1.5A	Micrograph of a high speed (12-in./sec) front contact laser scribe made on TCO/CdS/CIGS/Mo. (L903208b.jpg)5
1.5B	Perspective view of the front contact scribe showing selective removal of the TCO. (L903208c.jpg)5
1.6	SEM micrograph of a via scribe into TCO/CIGS. (L907411c).....7
2.1A	Micrograph of a line of insulating material using a new adhesive, printed at 12-in./sec. (I908401d).....10
2.1B	Micrograph of a line of insulating material using a previous formulation of adhesive, for comparison to Fig. 1A. (IJ199_1a)10
2.2	Perspective view a line of insulating material ink-jet deposited over a back contact scribe on CdS/CIGS/Mo/polyimide. (ij299_1c.jpg)11
2.3	Micrograph of a functional module interconnect incorporating the high speed scribing and ink-jet printing processes. (m91122a.jpg)12
3.1A	Plot of Cu film thickness vs. location on a 13-in. wide web.16
3.1B	CIGS film composition across the web width of a run made with a high Cu/(In+Ga) ratio.16
3.2A	Cu/(In+Ga) ratio of CIGS for two runs of 15m (upper plot) and 38 m (lower plot).16
3.2B	Ga/(In+Ga) ratio of CIGS for two runs of 15m (upper plot) and 38 m (lower plot).16
3.3	JV curve for a 9.8% efficient CIGS device on polyimide/Mo made in a small research system using the low temperature roll-to-roll process (measured at IEC).17

3.4	Auger depth profile of CIGS film made at low temperature with a web speed (metals and Se) of 6-inches/minute.	18
3.5	J-V characteristic of an 8.85% efficient device made at low substrate temperature on 13-in. wide web. Web speed for this device (metals and Se) was 6-inches/minute.	18
3.6A	Cross-section SEM of a CIGS film deposited in 12-inches/minute. (G147B_25).	19
3.6B	SEM of a CIGS film previously deposited at 6-inches/minute (G146).	19
3.7	The J-V characteristic of a small area device using an absorber layer deposited at 12-inches/minute. The efficiency of this device was 8%, measured at the IEC.	19
3.8	XRD spectra of CIGS material deposited at high deposition rates. The solid, short dashed and long dashed curves are for total deposition rates of 6, 12, and 18 inches/minute, respectively.	20
3.9A	Cu/(Ga+In) profiles for CIGS films with deposition rates of 6, 12, and 18 inches/minute.	21
3.9B	Ga/(Ga+In) profiles for CIGS films with deposition rates of 6, 12, and 18 inches/minute.	21
3.10	Impurities found by SIMS in CIGS films deposited at substrate speeds of 6, 12, and 18 inches/minute.	22
4.1	Raw SE Spectral Data Collected from Flexible CIGS films [Cu/(In + Ga) = 0.89]	27
4.2	Model of CIGS Samples used for Calculations.	28
4.3	The CIGS Spectral Fingerprint will be used to Design Interpretive Algorithms that Automatically Identify the Features of Interest.	28
4.4	A Representative Plot used to Generate the Quality Factor for each CIGS sample.	29
4.5	Application of the Quality Factors to CIGS Samples.	29
4.6	Conventional inverse parameter fitting method for determining properties.	30
5.1.	Representative I-V Curves for CIGS deposited at 400°C on Alternate Back Contact Materials.	38
5.2	Sheet Resistance as a function of distance a bi-layer back contact for a 150-ft roll-to-roll deposition trial.	40
5.3	SIMS Depth profile for CIGS deposited on a bi-layer back contact showing no interdiffusion between layers.	40
5.4	J-V for GSE Flexible CIGS Deposited on the Bi-layer Back Contact. The Figure Reveals an Ohmic Contact With CIGS.	41

List of Tables

<u>Table</u>		<u>Page</u>
1.1	EDS Analysis Showing Elements Present Before and After ITO Front Contact Scribing (10 keV Energy).....	6
4.1	Measured Ellipsometer Results from CIGS Samples. The band gap was calculated with the equation $E_g = 1.0032 + 0.71369y$, with $y = \text{Ga}/(\text{In} + \text{Ga})$; except a356, where the following equation was used $E_g = 1.011 + 0.664y + 0.249y(y-1)$. (Note: + = 'good', o = 'moderate', - = 'poor').....	28
5.1	Ohmic behavior of CIS/metal contacts from NREL Work [Ref 5-1]	34
5.2	Key material properties and cost estimates for alternative back contact materials proposed for an in-depth investigation under the GSE PVMaT program.	35
5.3	Key physical properties and Gibbs Free Energy Calculation for Reaction with Se at 400°C.....	35
5.4	Results of Alternative Back Contact Deposited on SLS glass.....	36
5.5	EDS composition Results for CIGS Deposited on Alternate Back Contacts.....	37
5.6	Summary of Device Results for CIGS devices deposited on Alternative Back Contacts.....	37

References

- [1-1] Private Communication, M. Contreras
- [1-2] M. Bodegard and L. Stolt, Proceedings of the 12th EC Photovoltaic Solar Energy Conference (1994) 1743.
- [1-3] V. Probst, J. Rimmasch, W. Stetter, H. Harms, W. Riedl, J. Holz and F. Karg, Proceedings of the 13th EC Photovoltaic Solar Energy Conference (1995) 2123.
- [5-1] R.J. Matson, O. Jamjoum, A.D. Buonaquisti, P.E. Russell, L.L. Kazmerski, P. Sheldon, and R.K. Arienkiel. Solar Cells. Vol. 11. 1984. 301

1.0 Task 1 – High Speed, All Laser Scribing Processes

1.1 Introduction

Monolithic integration divides active thin film PV into serially connected segments allowing the PV product to deliver an output voltage suited to an application. Serial interconnects are formed with three adjacent scribes in the back contact, absorber and front contact layers. Continuous scribes, yielding complete electrical interruption of the front and back contacts are required for the first and third scribes, without formation of bridging or shunts through the absorber layer. The second scribe forms a low resistance path between adjacent cell front and back contacts. From a manufacturing viewpoint, several areas are affected by scribing processes as described in the following paragraphs.

- **Manufacturing Rate Limitation** - Excluding module lamination and finishing, major steps that limit manufacturing throughput are often either the absorber deposition or the scribing operations for most thin film systems. Typical scribing equipment is limited to translation rates of 3 to 4-in./sec. Higher scribing rates coupled with multiple beam delivery are required to improve production throughput.
- **Active Area Loss** - Module efficiency is directly impacted by active area loss, which is related to scribe width and spacing. Scribe spacing is determined by the positional accuracy and minimum linewidths that can be obtained for the individual scribes. Accurate positioning registration, reproducibility and fine linewidth are required for both the laser scribing and printing steps to minimize active area loss.
- **Manufacturing Yield** - Product yield is a strong function of the control, reproducibility and robustness of the scribing process. The requirement for continuous front and back contact scribes is absolute. Defects caused by debris, or a single missed laser pulse can shunt an entire module segment, causing a measurable drop in performance and yield. Pinholes in the absorber, causing shunts, are often traced to debris or defect generation in the laser scribing processes. More obvious failures due to crossed or incomplete scribes also affect product yield loss. Debris must be minimized, and yield must be attacked by development of a broad, robust process window i.e., a tolerant process for each laser scribe, along with development of well-controlled, well-characterized equipment.

1.2 Task Objectives

The object of Task 1 is to develop the processes and equipment for selective scribing of device stack layers at high rates on flexible substrate.

Laser scribing is a major part of the patterning and integration process that enables module fabrication from a large area, thin film CIGS PV structure. Key issues with laser scribing are:

- Selective scribing of the thin film photovoltaics layers using all-laser methods,
- Avoiding shunt formation due to scribe debris or edge effects in a heat affected zone,
- Achieving scribe speed and multiple beam delivery which affects throughput, and
- Scribing process tolerance and robustness.

GSE is developing high throughput, all-laser processes for selective scribing of device layers. Goals of this GSE task are to:

- Develop a robust, selective processes for front contact, back contact and interconnect scribes to improve yield,
- Develop the equipment and methods to increase scribing speed to 23 cm/sec to improve throughput, cost and reduce capital investment, and
- Minimize scribe debris, scribe width and heat affected zone adjacent to scribe.

1.3 Technical Approach

It is advantageous in roll-to-roll processing of flexible substrates to avoid mechanical scribing steps and to scribe exclusively from the front side of the thin film structure. Accordingly, GSE is developing all-laser, multiple beam scribing processes using radically different laser equipment than that traditionally used for monolithic integration of thin-film PV modules.

Dedicated equipment specially designed for high speed, high accuracy laser scribing over large areas was assembled. The new laser scribing station at GSE incorporates capabilities for roll-to-roll web transport and tensioning across a working surface, automated machine vision and inspection, compact generation and delivery of multiple laser beams, and accurate, high speed motion control of the beams relative to the substrate in 3 dimensions.

Process parameters needed to obtain clean scribes selectively in each layer at high speeds are under development. The impact of the scribing parameters (feed rate, power, wavelength, focus spot size and spot overlap) and substrate related parameters including layer type, thickness and composition on shunting, debris generation, scribe quality and characteristics must be determined.

1.4 Results

1.4.1 Equipment Status

GSE has designed and built a high rate, pilot production laser scribing station. Key features of this system include components for high speed, accurate motion, machine vision, beam delivery optics, web transport and control and a rigid support structure.

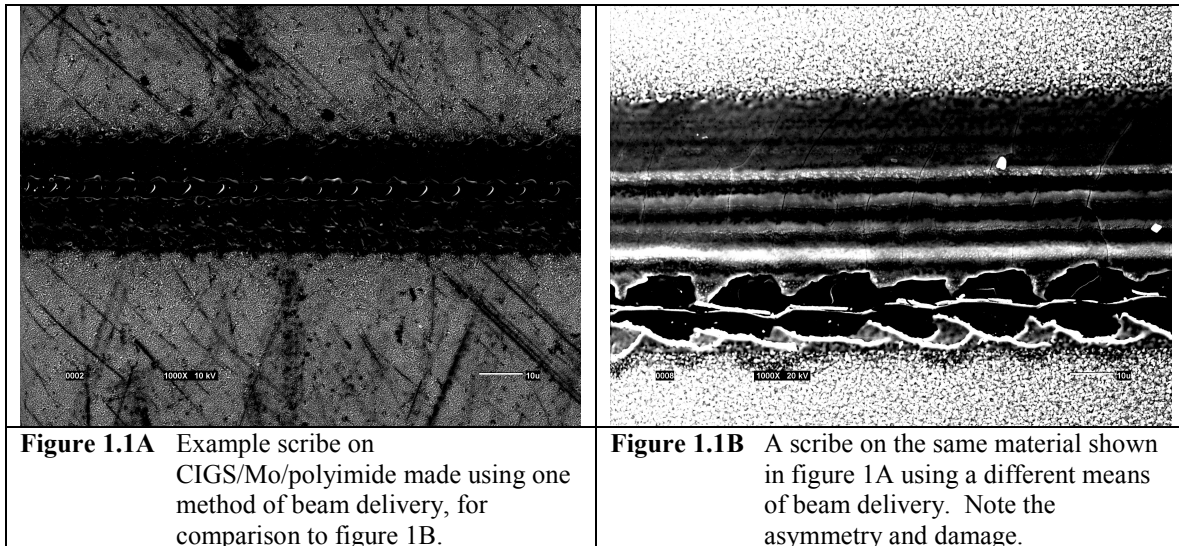
Controlled X-Y motion of the optics head has been demonstrated over a 16x40-in. area at speeds from 12-in./sec to 24-in./sec concurrent with a positional accuracy and reproducibility of 10 microns. These conditions meet or exceed the anticipated requirements for high speed scribing for throughput goals and accuracy requirements to minimize module area loss.

The web transport system has been developed to maintain the flexible substrate very flat on a platen during scribing operations. A very flat web surface is necessary for accurate z-axis focus. Maintaining accurate z-axis focus is complicated by intrinsic stresses in the thin film contact and absorber layers, which introduce a natural curl in the web. Several innovations have greatly improved our capability for web flatness, even with highly stressed substrates.

Machine vision components, including a fast analog camera, a high resolution digital camera, board-level machine vision processors and software have worked well to locate fiducials on a panel, achieve pattern registration, compensate automatically for web alignment errors and allow detailed visual inspection of scribe characteristics during processing.

Several methods and variations of beam delivery were evaluated to optimize the delivered beam characteristics, size, and overall power transmission efficiency. Elimination of non-uniform or undesirable beam intensity distributions and modes was particularly important to obtain clean, controllable scribes.

Figures 1.1A and 1.1B, which show laser scribes made in CIGS but using different beam delivery methods, illustrate the impact of beam delivery on scribe characteristics. Various problems, including excessive damage, debris and asymmetry can be caused by improper beam characteristics.



1.4.2 Scribe Interconnect Development

The scribe methodology selected for interconnection of module segments on flexible polyimide substrates is illustrated in Figure 1.2 and the resulting in the interconnect structure shown in Figure 1.3. As shown, the back contact scribe must be accomplished first by selectively cutting through the CdS, CIGS and Mo back contact, leaving the polyimide substrate intact. Concurrently, the via is formed by selectively scribing through the CdS and CIGS, but not through the Mo. After, the via and back contact scribes are complete, the back contact scribe is filled with insulative ink to avoid shunting between the front and back layers as well as to avoid reconnection of adjacent back contact pads during TCO deposition. Finally selective scribing of the TCO is conducted completing the serial interconnection of adjacent thin film cells.

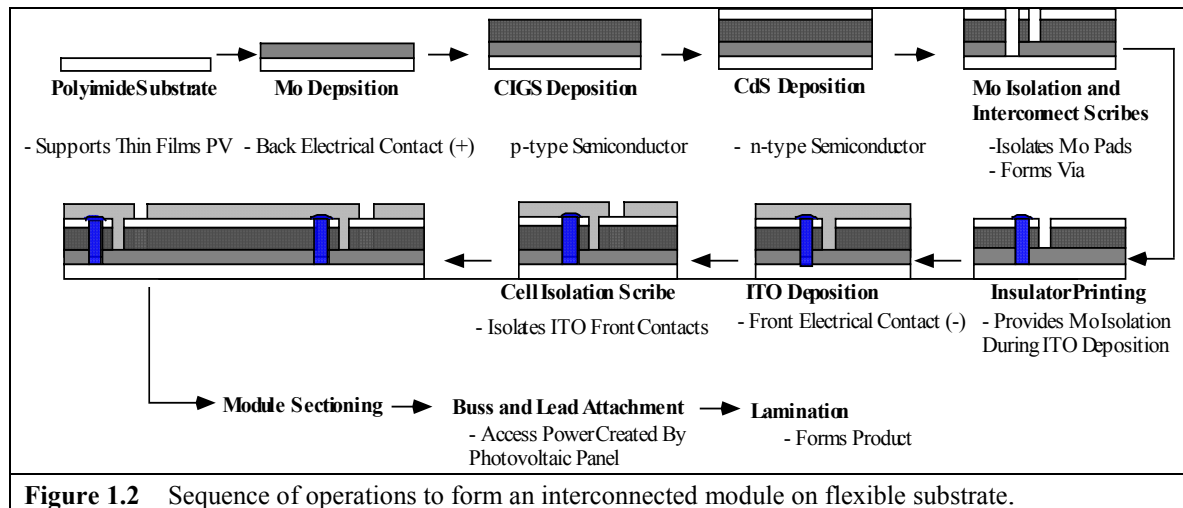


Figure 1.2 Sequence of operations to form an interconnected module on flexible substrate.

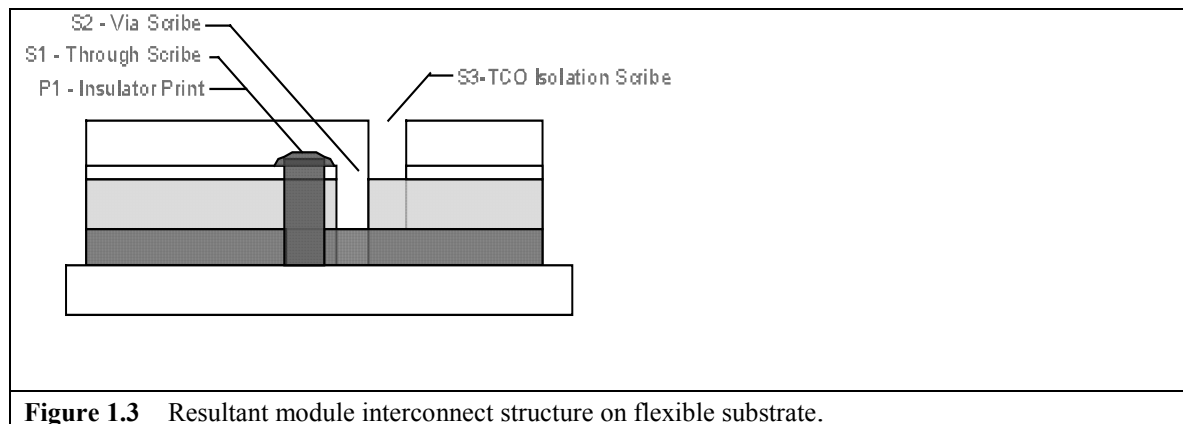
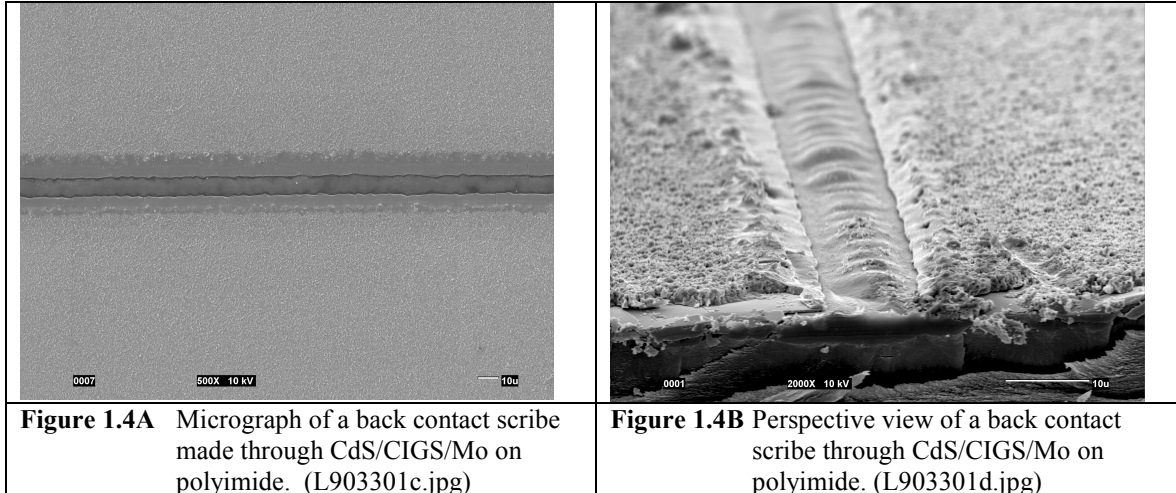


Figure 1.3 Resultant module interconnect structure on flexible substrate.

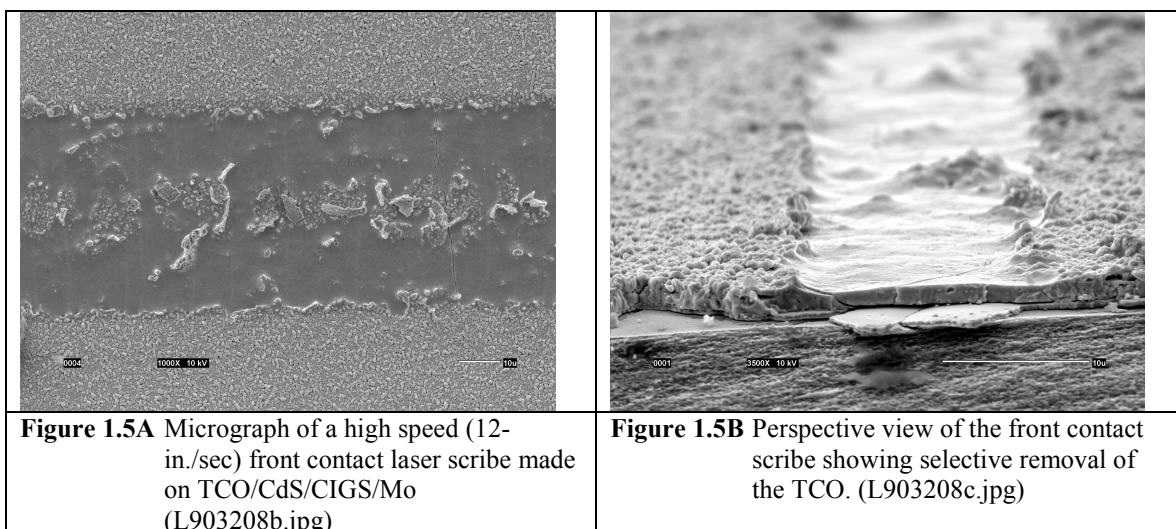
1.4.2.1 Back Contact Scribe -- Parameters were developed to produce selective cutting of the CdS, CIGS and Mo back contact down to the polyimide. Figure 1.4A and 1.4B show representative back contact scribes. Melted material removed from the scribed area is visible as a berm along the scribe edges. Fortunately there is little tendency toward formation of loose debris or asperities which may cause shunts. Selective cutting is evident in Figure 4A and 4B as the CdS, CIGS, and Mo are removed, leaving the underlying polyimide surface relatively intact. The scribing rate for the back contact scribe developed at GSE is 12-in./sec, which exceeds the

end-of-contract goal for the PVMaT initiative (9.1 in./sec). Moreover, this back contact scribe process has been verified electrically, indicating a high resistance from segment-to-segment. Failure rate in brief trials was less than 0.5%, most likely due to a bridging defect or ambient surface debris that blocked the beam.



1.4.2.2 Front Contact Scribe -- Development of a laser process for the front contact of the CIGS structure represents a challenge in that laser ablation must fully remove the TCO, yet abruptly stop before the back contact is damaged. Selective cutting is difficult because all layers are thin compared to the scribe width and the layers are thermally and mechanically well coupled. Moreover, the CIGS and back contact layers rapidly absorb most laser wavelengths that are well absorbed by the TCO.

Promising selective scribing results were achieved showing preliminary feasibility of a laser process for front contact scribing. Typical scribe morphology results are shown in Figure 1.5A and 1.5B.



Selective removal of the TCO layer (granular, small featured material on top) appears evident, particularly in Figure 1.5B. The CIGS underneath appears to be largely intact after front contact scribing. Elemental analysis by EDS at low acceleration voltages (10 keV) is shown in Table 1.1 for regions inside and immediately outside the high-speed front contact scribe. In this case the predominant EDS signals outside the scribe are Sn and In from an indium-tin oxide (ITO) front contact and Cd and S from the underlying CdS heterojunction layer. After scribing, the tin (Sn) signal is essentially gone and Cu, In, Ga and Se signals from the CIGS absorber became predominant. Small signals from residual remaining Cd and S were also evident, possibly indicating the selective scribe did not fully remove the CdS layer.

Table 1.1 EDS Analysis Showing Elements Present Before and After ITO Front Contact Scribing (10 keV Energy)

	Outside Scribe (elemental %)	Inside Scribed Area (elemental %)
Cu	0.45	24.16
In	80.46	19.93
Ga	0.25	6.15
Se	0.54	45.05
Cd	5.40	2.22
S	3.10	1.24
Sn	8.23	0.37

Absolute composition can not be inferred from the data in Table 1.1, as the low accelerating voltage used to maximize the surface sensitivity of the EDS analysis precludes accurate analysis for some elements due to insufficient peak excitation or peak overlap.

As with the back contact scribe, GSE has accomplished the front contact scribe at a rate of 12-in./sec (30.5-cm/sec), which exceeds the PVMaT end-of-contract goal of 9.1 in./sec. (23-cm/sec)

1.4.2.3 Interconnect (or “via”) Scribe -- A high speed (12-in./sec) laser process has also been developed by GSE that may be suitable for a low resistance interconnect between module segments. Figure 1.6 shows material that was scribed using conditions to selectively cut through the CdS and CIGS layers to expose the back contact layer. EDS analysis revealed undisturbed CdS/CIGS at location ‘A’ in Figure 1.6. Inside the scribe at location ‘B’ the CdS/CIGS was largely removed with only a thin layer of CIGS remaining. At locations ‘C’ and ‘D’ in Figure 1.6, EDS analysis revealed exposed back contact and substrate material, respectively.

Unlike the front and back contact scribes, the via scribe need not be continuous, and it appears that a low resistance path between the back and front contact may be formed in areas ‘B’ and ‘C’ of the scribe.

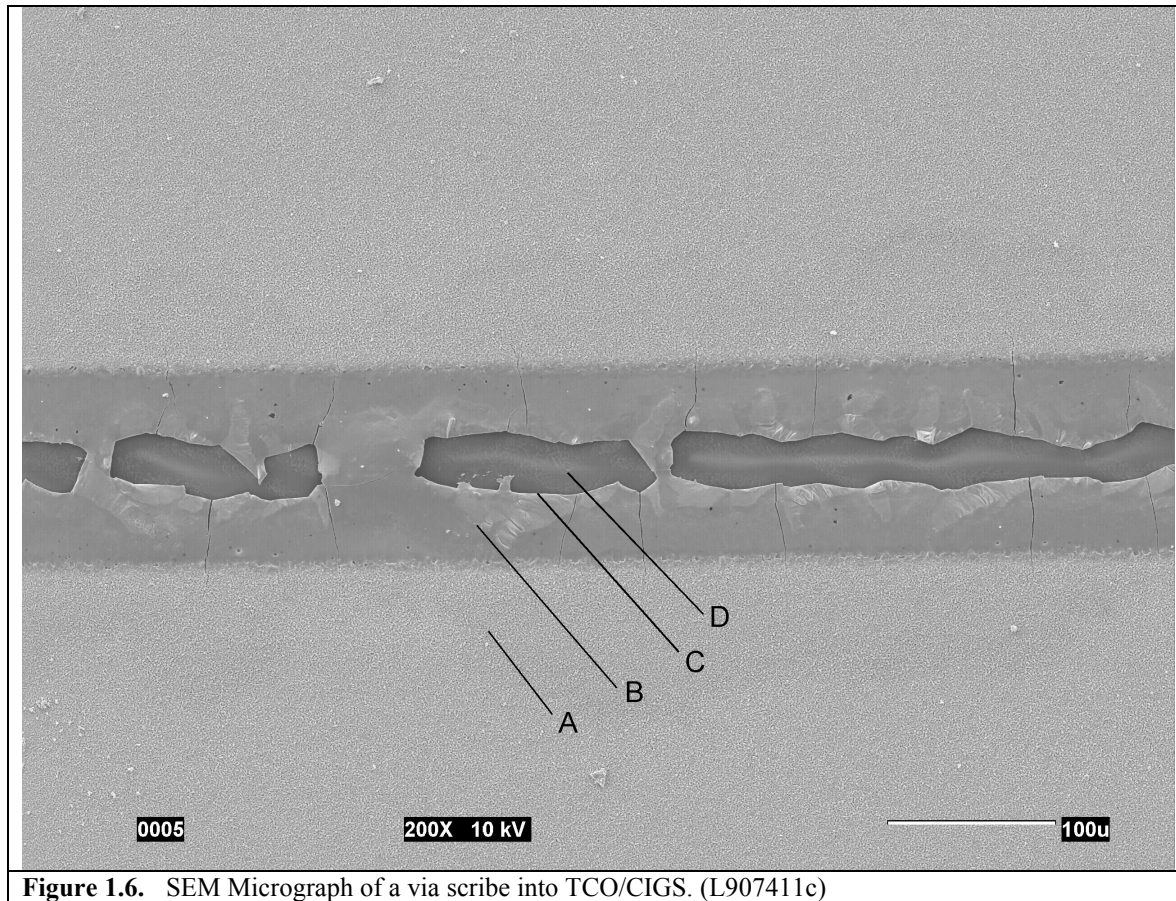


Figure 1.6. SEM Micrograph of a via scribe into TCO/CIGS. (L907411c)

1.5 Conclusions and Future Work

GSE has successfully developed conditions and equipment that appear to produce viable, all-laser, high speed (12-in./sec, 30.5-cm/sec) processes for the back contact, front contact and interconnect scribes for CIGS based modules on flexible polyimide substrates. High rate, selective, thin film cutting has been evidenced for these process, and all scribe processes have been validated microstructurally by optical and SEM examination. The high rate back contact scribing process has also been validated through electrical tests. High rate front contact and interconnect scribe remain to be validated by electrical tests, and further optimization will certainly be required based on electrical test results. Robustness, sources of variability and process sensitivity also remain to be fully evaluated. Scribe widths may eventually be minimized as well.

Some further equipment modifications are planned, including improved web transport tensioning and accuracy, software control, some speed improvements to the motion system and some changes to the high resolution portion of the machine vision system.

2.0 Task 2 – Ink-Jet Technology for Insulator Deposition in Scribes

2.1 Introduction

The post-absorber laser scribing approach described in the last section requires that an insulating material be deposited over the back contact scribe, preventing direct shunt formation upon subsequent deposition of the TCO front contact. Screen printing is the technique conventionally used to deposit insulating material in the scribe, but suffers from several drawbacks. Silk screen printing typically produces 250 to 1000 micron linewidths, which would cause significant module area loss. Additionally, the screens stretch with use, causing registration errors and further loss in module area and manufacturing yield. Silk screen printing is also inflexible in that even small pattern changes require fabrication of completely new screens.

Ink-jet technology was proposed as a method for controllably printing scribe areas with insulating lines while circumventing the limitations of screen printing. Conceptually, a single head capable of controllably dispensing a fine line of insulating material could be positioned and moved rapidly over a substrate area to generate a printed pattern.

Several types of ink-jet technologies exist, including “bubble-jet”, electrostatic/ultrasonic ink drop, and valved fluid dispense through an orifice. Each method is constrained by different limitations, such as speed, ultimate linewidth, or required fluid characteristics. For instance, the electronic/ultrasonic ink drop delivery is capable of very high printing speeds, but can dispense very limited types of fluid, having strict requirements on viscosity, surface tension, electrical conductivity and vapor pressure.

Drying or curing time is also an important parameter for the printed insulator materials, as rapid processes for module production are needed for high throughput. Success in this task depends on developing the equipment and process for rapidly depositing and drying insulating ink that is compatible with subsequent processes.

2.2 Task Objectives

The challenge in this task is to adapt commercially available ink-jet technology to PV module manufacturing. Key advantages of ink jet include reduced area loss, increased pattern accuracy, and improved pattern flexibility over the baseline process of screen-printing. Key issues with ink-jet insulator deposition are:

- Printing fine-width, accurate lines,
- Achieving continuous and uniform lines,
- Determining parameters for high rate deposition and post-deposition curing,
- Identifying insulating materials that are compatible with subsequent PV module manufacturing processes,

- Identifying insulating materials with low outgassing, good adhesion, minimal shrinkage, and high resistivity.

Key goals in developing ink-jet technology under this task include:

- Developing parameters to achieve reproducible, continuous, well adherent lines of insulating material with uniform linewidths.
- Obtaining progressively decreasing linewidths, to 125 microns, maintaining line continuity and uniformity.
- Developing the equipment and methods to minimize drying time and enable deposition rates of 8.7 in./sec.
- Assuring compatibility and integrating the ink jet with all other module fabrication processes.

2.3 Technical Approach

Commercially available techniques for ink-jet printing were surveyed, including bubble-jet or “drop-on-demand”, electrostatic/ultrasonic continuous print, and valved fluid dispense through an orifice. The most promising method was selected by matching the capability of the technology to the expected requirements for PV module manufacturing. Factors such as line printing speed, accuracy and ultimate printed linewidth were considered in addition to the properties of the inks that could be used with each technique, such as drying time, adhesion, temperature limit, outgassing and shrinkage.

Commercially available ink-jet equipment was obtained, modified where required, and integrated into the GSE high-speed scribing station. The ink-jet head itself was mounted on the flying optics head, allowing rapid positioning and linear movement to a 10 micron accuracy over a 16-in. x 38-in. module processing area. Independent means to control the z-axis position, or height of the dispense tip from the module surface were also installed, along with associated valving, fluid delivery and control functions.

Printed ink patterning was controlled by the same software used for laser patterning. Special provisions were made for rapidly drying the deposited ink pattern after it was deposited, and before it was rolled onto a take-up mandrel. Subsequently a new section of 13-in. wide web would be rolled out from the pay-out mandrel onto the working platen for ink-jet patterning.

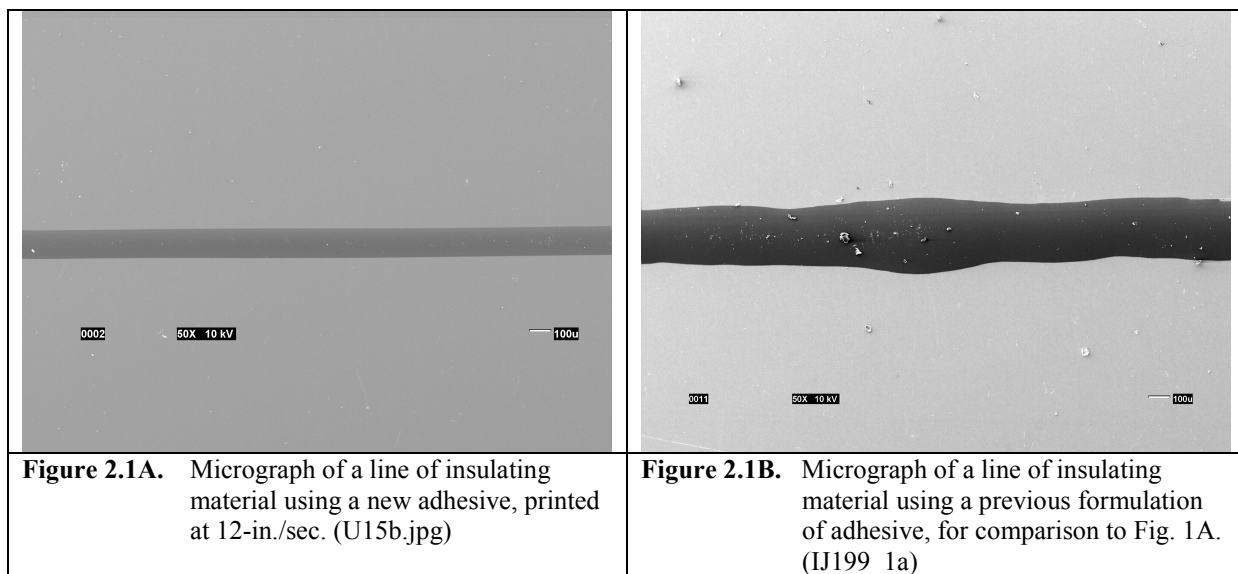
2.4 Results

The high speed scribing station at GSE was fitted as described with commercially available ink-jet equipment, and many sequences of tests were run to deposit ink patterns on several different substrate materials. Important process variables were identified, including fluid viscosity and type, ink-jet deposition rate, substrate-to-dispense head distance, substrate type and others.

Initially a host of difficulties were encountered, such as excessive linewidths, non-reproducibility, and uniformity in printed lines. Overall process speed, one of the major requirements under the PVMaT initiative did not meet requirements, mostly due to a lengthy ink curing time. Process and equipment robustness were also early problems. For example, printed linewidth was found to strongly depend on substrate type. Linewidths were much greater on CIGS compared to molybdenum coated polyimide. Ink spreading was presumably impacted by the different surface energy or capillary action of a microscopically textured polycrystalline surface. Ink spreading, and thus printed linewidth, was also a strong function of the ink type.

2.4.1 Linewidth Improvement

Figure 2.1A and 2.1B illustrate the effect of ink type on linewidth and line uniformity. The ink used for the line in Figure 2.1A allows a much thinner and more uniform line to be printed.



Linewidths progressively decreasing to 125 microns for the printed insulating material is one goal of the PVMaT contract. Significant progress has been made in reducing printed linewidths. Linewidths of about 200 microns are routinely achieved, and lines less than 100 microns wide have been produced at GSE, exceeding the end-of-contract goal. However, process reproducibility and control is not yet sufficient to print lines thinner than 150 microns on a routine basis. Most of the improvement in linewidth resulted from improvements to the ink-jet equipment and the selection of more suitable inks. Some of the non-uniformity in the printed line was also due to voids and bubbles in the fluid, and has since been eliminated.

2.4.2 Process Speed, Compatibility

PVMaT goals oriented toward high speed processes stipulate that the ink print process attain rates of 22 cm/sec. Near the start of Phase 1 the entire process was limited by the ink curing time to an overall rate that was almost an order of magnitude too slow. Selection of rapidly curing inks and innovations at GSE has dramatically improved the speed of the ink printing process. As a result, the ink curing process is no longer rate limiting. Ink line printing rates of

12-in./sec (30.5-cm/sec) are routine, exceeding the end-of-contract goal of 22-cm/sec for ink line printing speed. To date, groups of up to 100 consecutive lines of insulating material were ink-jet printed without skips or defects at the 12-in./sec (30.5-cm/sec) rate.

Adhesion has not been a problem to date, as most of the ink types and conditions have produced very well adherent insulating material. Figure 2.2 shows a crosssectional view of a typical ink-jet deposited insulating line. In this case, the ink line is deposited directly over a back contact scribe, although that scribe is not visible.

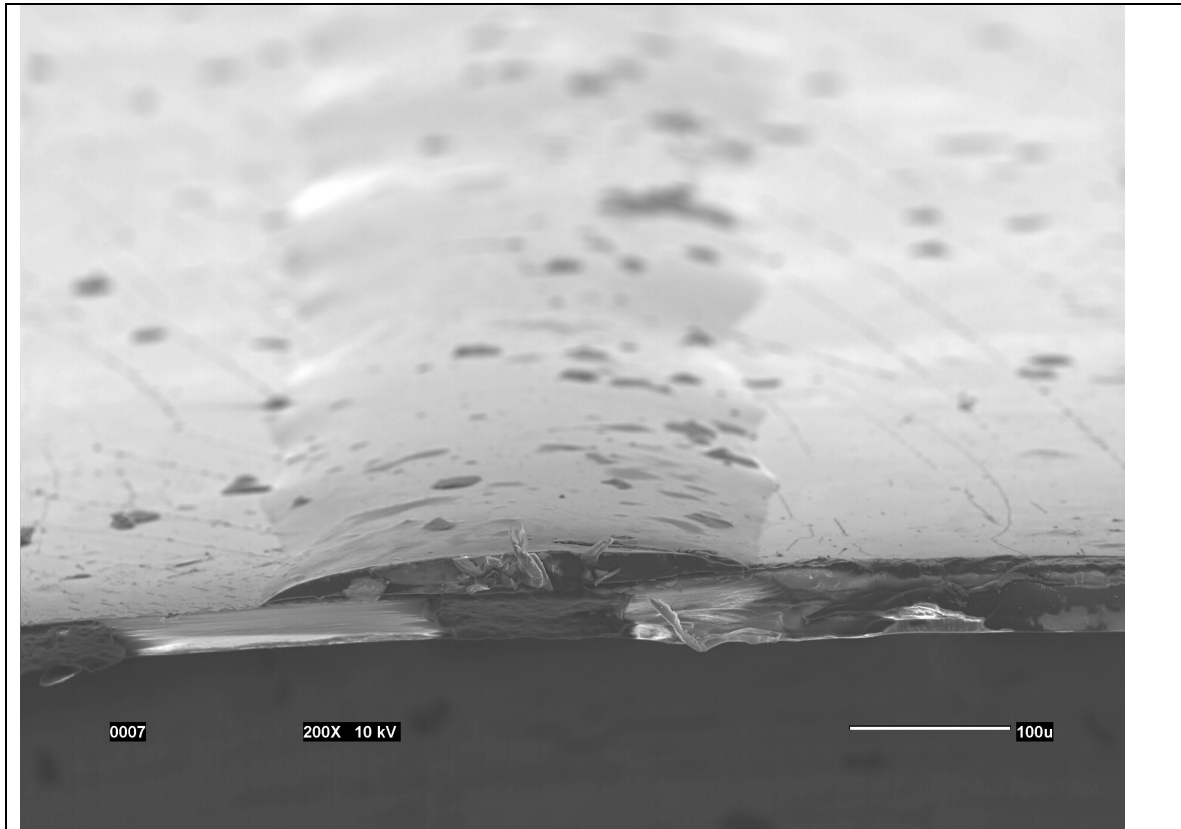


Figure 2.2 Perspective view a line of insulating material ink-jet deposited over a back contact scribe on CdS/CIGS/Mo/polyimide. (ij299_1c.jpg)

Process compatibility problems in the subsequent TCO deposition process, either due to outgassing or temperature induced degradation of the insulating material, have not been fully determined.

Figure 2.3 depicts a module interconnect, showing (from left to right) the front contact scribe, interconnect or “via” scribe, and the printed line of insulating material. The location of the back contact scribe is visible under the printed ink line, and the horizontal scribe in the micrograph is a termination scribe to define the edge of the module active area (also made through a line of printed insulator). For diagnostic purposes, the scribe spacing is intentionally farther apart than normally desirable. Also, for test purposes the printed ink line is not centered over the back contact scribe. Module interconnects, made entirely with high speed processes, such as those in Figure 2.3 were used to fabricate functional modules. Loss analysis has not been completed on

those modules, however in many cases the monolithic interconnects produced serial addition of segment voltages apparently with negligible loss due to shunts or other problems.

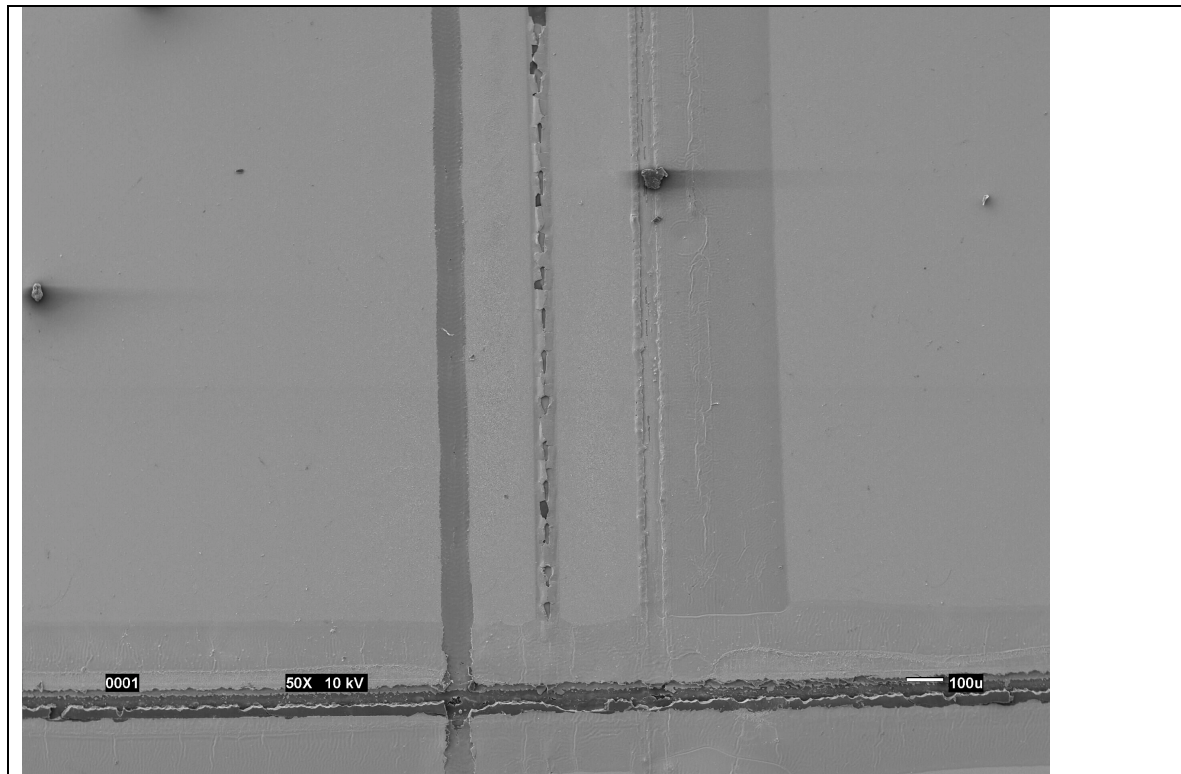


Figure 2.3 Micrograph of a functional module interconnect incorporating the high speed scribing and ink-jet printing processes. (m91122a.jpg)

2.5 Conclusions and Future Work

The ink-jet deposition of insulating material in back contact scribes appears to be a viable and compatible process. PVMaT end-of-contract goals for process speed have already been exceeded, and have been approached for printed line width and uniformity. Full scale manufacturing using the high speed process will demand some further improvement in process reproducibility. Further equipment modifications to improve control and reproducibility, and ease of set-up are planned. Subsequently, process sensitivity and tolerance will be more thoroughly evaluated. Printed linewidths will be further reduced, and scribe spacing will be compressed to minimize loss of active area.

3.0 Task 3 – High Rate CIGS Deposition

3.1 Introduction

One limiting factor for PV module throughput, and subsequent cost, is the absorber deposition. Neither the equipment nor the proof of concept exist for very high rate CIGS deposition for use in large area thin film PV manufacturing. The challenges in this task are the high rate, controlled, simultaneous delivery of Cu, In, Ga and Se to the substrate surface under conditions that form a dense, stoichiometric, well adherent film of high quality CIGS. Issues including control of the Ga concentration, as well as Ga concentration profile to control absorber bandgap, impurity and defect densities, morphology, grain boundaries and surface termination are all critical to absorber layer quality, and thus also to device and module performance.

For co-evaporation processes the kinetic rate limitation on CIGS compound formation is not known. Generally high quality CIGS has been formed at relatively slow rates (>30 min. deposition time). However, work in some laboratories using elemental co-evaporation at high substrate temperatures (>500 °C) indicates that a high quality CIGS absorber layer can be formed using 5-10 min. for the metals delivery. [3-1] High rate deposition bodes well for a rapid manufacturing process, however, the manufacturing process used at GSE introduces several additional constraints. Large area, uniform deposition of CIGS must be accomplished at GSE with process temperatures less than about 400°C because higher temperatures degrade the flexible polymer substrate. Consequently, mixing and mass transport that are dependent on diffusion are much reduced compared to the diffusive rates that exist at much higher temperatures when CIGS is grown on glass substrates. Moreover, the intrinsic source of sodium associated with glass substrates is unavailable when using polymer substrates. Sodium incorporation has been shown to improve absorber quality and spatial uniformity of the photoresponse. [3-2, 3-3]. The formation of CIGS at high rates, with low temperatures and on polymer substrates is unexplored.

Photogeneration and charge collection take place in CIGS absorber layer and so it is central to photovoltaic performance. Electronic properties such as carrier concentration and mobility, defect densities, minority carrier lifetime and internal electric junction field strength are critical. Along with the above mentioned electronic characteristics, physical aspects such as adhesion and continuity of absorber coverage have dramatic effects on final module performance. The absorber deposition process must yielding high quality material, be economical, fast, controllable and scaleable to large area.

One additional consideration for manufacturable absorber processes is selenium utilization. Although excess of Se is provided in laboratory systems to enhance CIGS growth, a 3 to 4 times stoichiometric excess of Se for continuous operation of in-line CIGS systems may increase downtime for clean-up and costs associated with waste disposal.

3.2 Task 3 Objectives

High rate deposition of the absorber layer is essential to raise throughput and reduce cost for manufacturing thin film CIGS PV modules. GSE is using large area co-evaporation of elemental

constituents in a continuous, roll-to-roll method to form the thin film CIGS absorber. Key issues with CIGS deposition are:

- Evaporative sources capable of uniform, controllable, high rate delivery of reactants over a large area.
- Electronic quality and adhesion of CIGS deposited at high rate, with the constraint of a low substrate temperature process.
- Source heat dissipation to web and chamber.
- Materials utilization, Se delivery and system maintenance/downtime.

GSE is developing the equipment and methods for CIGS absorber deposition at high rate. Key goals of this task are:

- Develop evaporative sources capable of uniform, controllable, high rate delivery of reactants over a large area.
- Evaluate CIGS absorber quality at progressively higher deposition rates, up to 27 cm/minutes web speed (a 100 % increase over base rate).
- Develop methods for deposition of adherent, high quality CIGS at high rates and low substrate temperature.
- Demonstrate module production using the high rate process, incorporate high rate absorber deposition methods and equipment into the GSE manufacturing line.
- Maximize Se utilization, thus decreasing Se consumption and required downtime for system cleaning and maintenance.

3.3 Technical Approach

The baseline GSE CIGS manufacturing process consists of direct co-evaporation from elemental sources and was selected over sequential based sputtering processes because:

- Co-evaporation allows direct gallium incorporation into the active region of the absorber even at low substrate temperatures resulting in higher bandgap, and thus higher voltage per module segment.
- Substantially reduced cost because of high materials utilization (70 to 80% compared to 20 to 30% for sputtering) and low cost starting materials.
- Ability to produce quality stoichiometric and off-stoichiometric compounds (i.e., transition from Cu-lean to Cu-rich and back Cu-lean within a single deposition zone).
- Process throughput for direct co-evaporation is much higher because finishing heat treatments are not necessary, and capital cost for the required deposition equipment is significantly lower.
- Direct co-evaporation from elemental sources has higher materials utilization and avoids source material fabrication costs associated with making and bonding sputtering targets. These avoided costs and speed advantages take on extreme importance in a manufacturing environment.
- Compared to the elemental sputtering/selenization, direct co-evaporation has yielded CIGS material of better quality, evidenced by devices having higher efficiency.

For large-area, high-rate vapor phase manufacturing of compound semiconductor devices, multi-source evaporation on a moving substrate (flexible or rigid) provides the best combination of performance and low-cost.

Source modeling was conducted to optimize materials utilization while achieving a uniform thickness across the web. Down web composition uniformity is achieved by the web movement through a well defined deposition zone at a constant speed. Modeling indicated that high source utilization (>60%) required a relatively close source-to-substrate spacing.

GSE has designed and built continuous roll-to-roll CIGS deposition systems using multi-source co-evaporation in which substrate is transported above sources operated at a constant flux. With specific spacing between the sources, the web motion creates a controllable flux profile at the substrate. Using a GSE roll coating system, adherent, uniform, stoichiometric CIGS has been deposited that is single phase and has large grains.

3.4 Results

3.4.1 Source Design

Many extreme requirements exist that critically affect source design, the most obvious being high temperature operation for extended periods of time, material flux delivery that is uniform and well controlled, and limited heat dissipation to surrounding parts. At GSE we have taken innovative approaches toward meeting all the requirements for operational sources. Multiple iterations of source design or modification followed by evaluation were required to meet all of the technical challenges. Some of the technical requirements of source design are mutually conflicting, thus compromises to satisfy design issues to a satisfactory level had to be worked out.

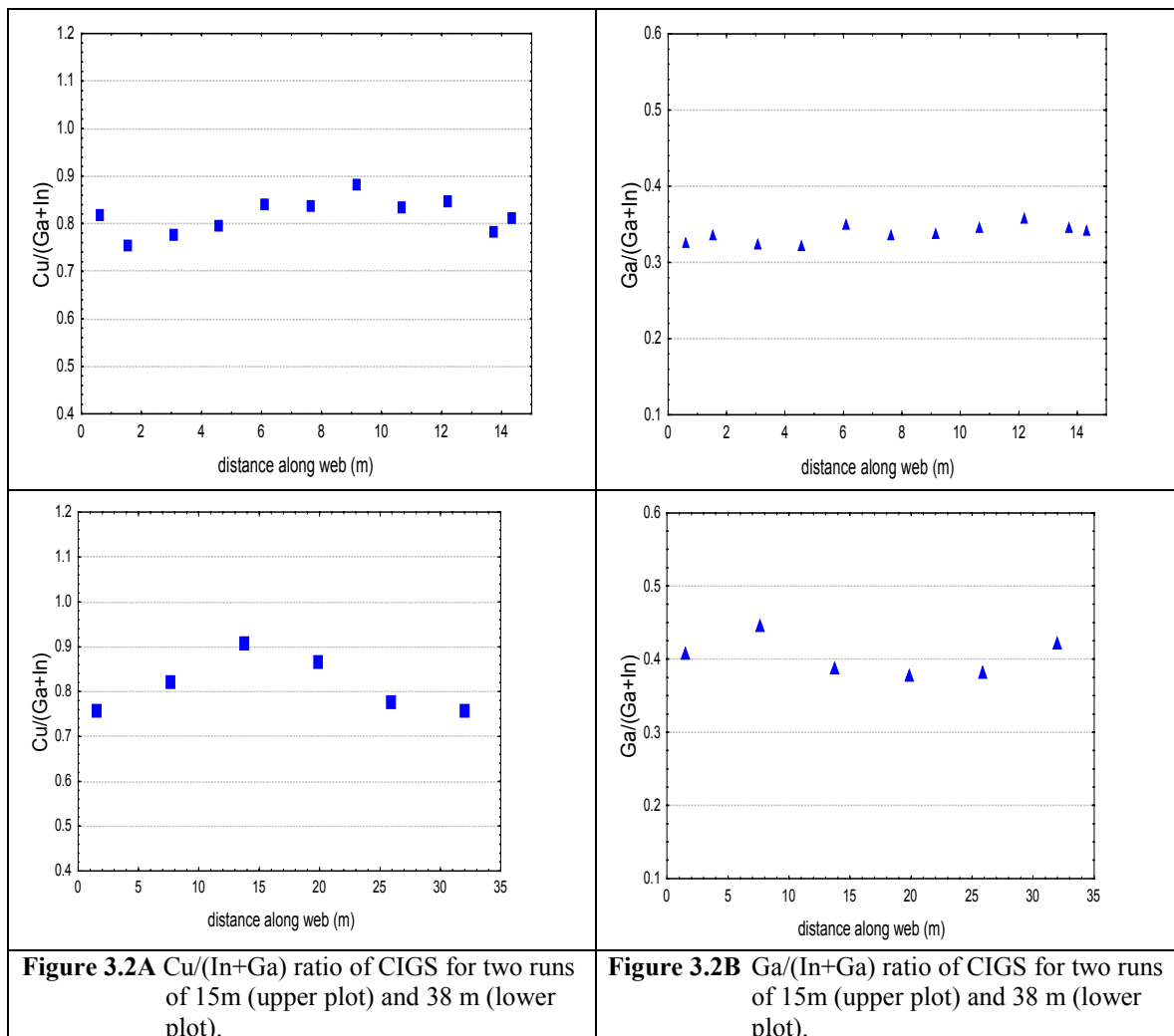
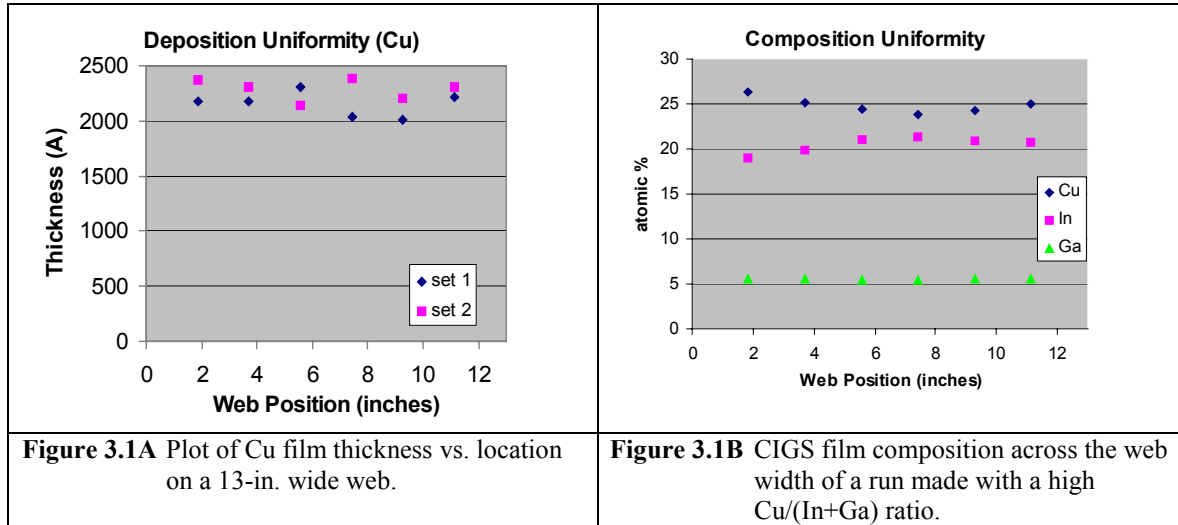
Much progress has been made, and sources are operational at GSE for high rate, uniform delivery of Cu, In, Ga and Se. Even so, further improvements to the source design are expected on an evolutionary basis.

3.4.2 Materials Flux Uniformity

Figure 3.1 shows the uniformity obtained across the width of a 13-in. web for Cu deposition only in two separate runs. Much of the variation present is due to measurement error on the flexible substrate. Material thickness uniformity across the web width with less than 10% variation should be possible. However, some variation in the In profile can occur, yielding a variation in Cu/(In+Ga) ratio that is more than 10% from center to edge. If the variation across the web is severe, portions of the film can become Cu-rich, as illustrated in Figure 3.2. Improved uniformity is expected after minor modifications in source design have been implemented.

Material uniformity as the run progresses (down the web) is also important for yield and efficiency considerations. Figure 3.2A and 3.2B show measurements of CIGS composition as a function of run time or web length, indicating variation in Cu/(In+Ga) ratio and Ga/(In+Ga) ratio. Composition variation of this magnitude, or greater was expected, and was a primary

reason for development of an in-situ diagnostic capability described under Task 4. The CIGS material of Figure 3.2A and 3.2B was deposited without any active control or in-situ diagnostic.



3.4.3 CIGS Material Quality Using a Low Temperature Process

Using the sources developed at GSE, CIGS of reasonable quality was produced in a continuous (roll-to-roll) process on Mo/polyimide substrates, as shown by device efficiencies of 9.8% (Figure 3.3). The device represented in Figure 3.3 was made in a small research system from a low temperature process and contains no sodium, in contrast to devices typically made on glass.

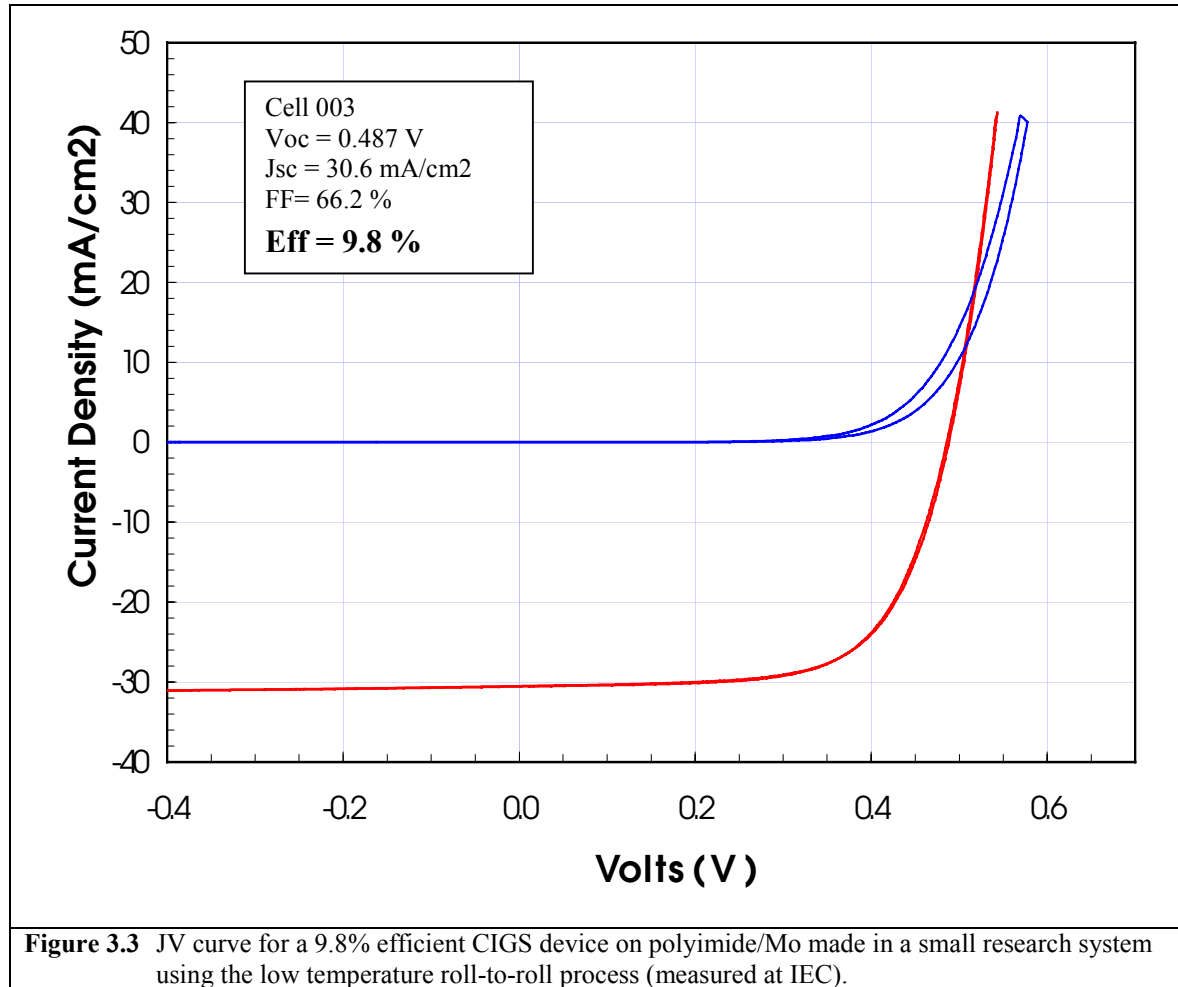


Figure 3.3 JV curve for a 9.8% efficient CIGS device on polyimide/Mo made in a small research system using the low temperature roll-to-roll process (measured at IEC).

Compositional uniformity through the film thickness is a serious issue. The rapid film growth rates and low substrate temperatures required for high rate manufacturing on the flexible web limit both the time and temperature normally available to assure thorough mixing and reaction through diffusion.

However, in production-based equipment using total deposition time that corresponds to a web speed of 6-inches/minute at substrate temperatures near 400°C fairly uniform compositional profiles through the thickness were achieved, as shown in Figure 3.4. Presently the last grown material (near the surface) still shows a gradient in Ga/(In+Ga) that is larger than desired. Modifications are planned to further alleviate compositional gradients. At the baseline rate that corresponds to a web speed of 6-inches/minute for the CIGS layer, device performance of up to 8.85% (shown in Figure 3.5) has been achieved in the production-based equipment.

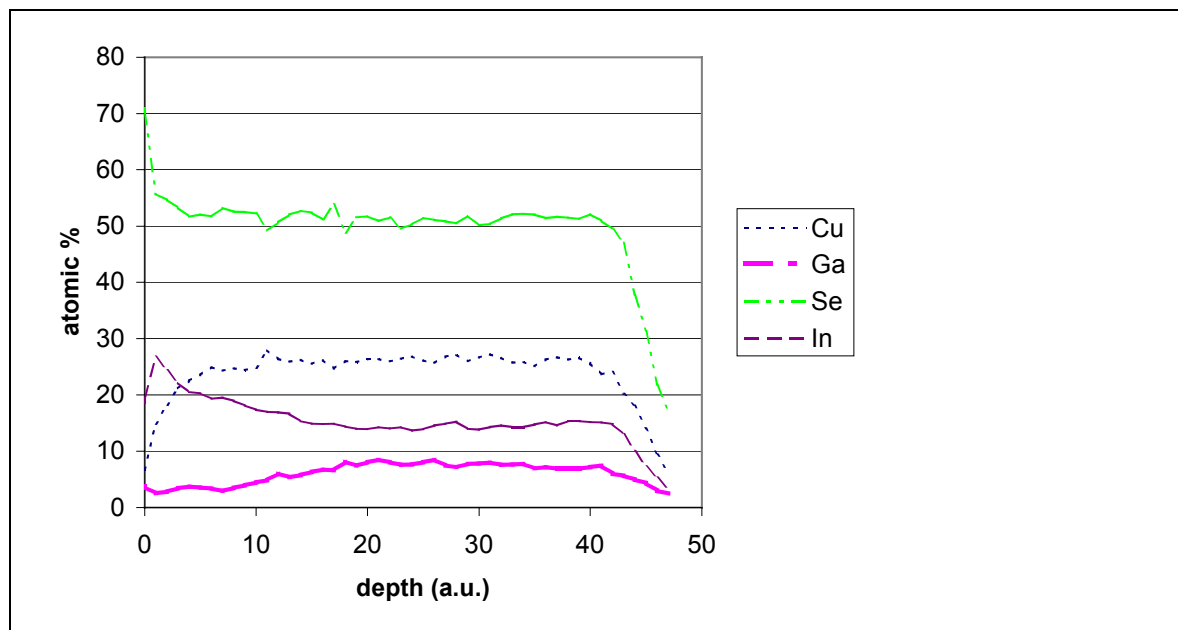


Figure 3.4 Auger depth profile of CIGS film made at low temperature with a web speed (metals and Se) of 6-inches/minute.

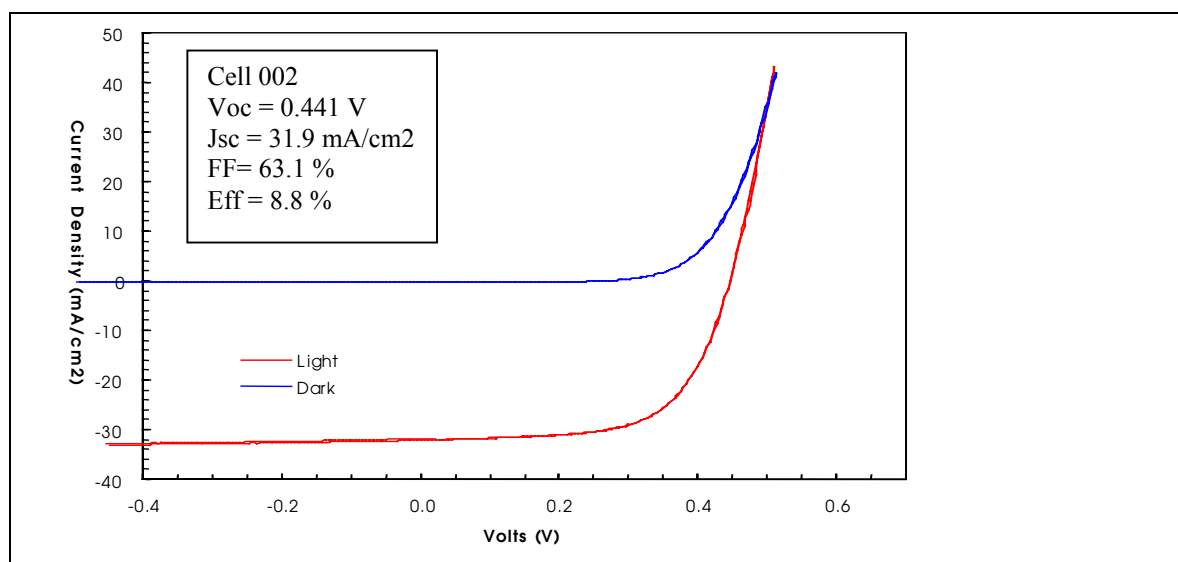


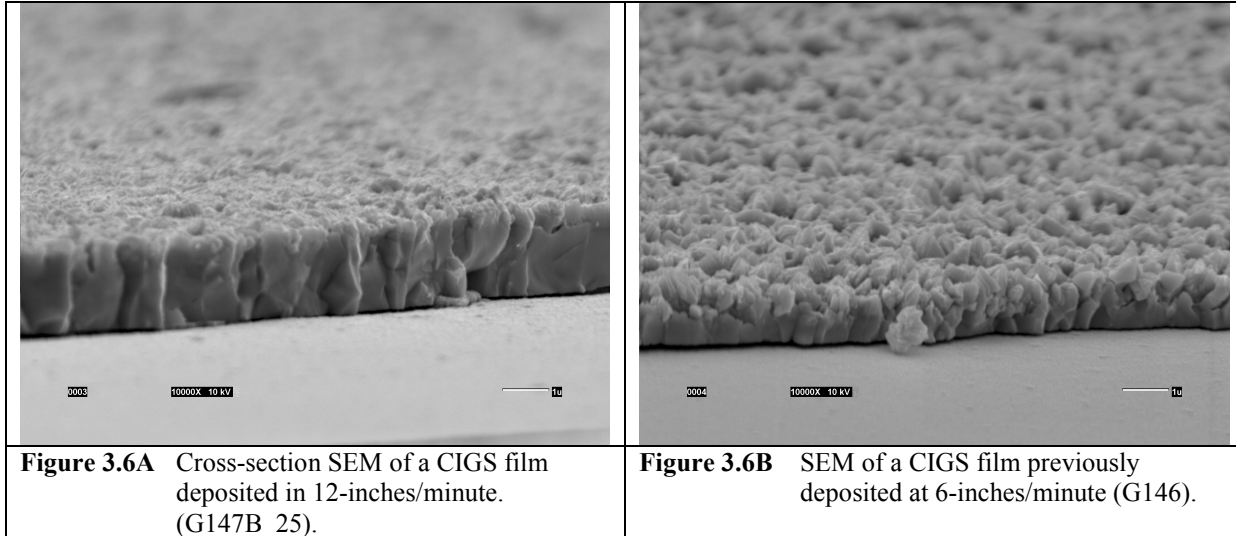
Figure 3.5 J-V characteristic of an 8.85% efficient device made at low substrate temperature on 13-in. wide web. Web speed for this device (metals and Se) was 6-inches/minute.

3.4.4 High Rate CIGS Deposition

We have deposited CIGS at web speeds of up to 24 inches/minutes. It should be noted that the deposition rate includes the metals deposition (Cu, In and Ga) and exposure to Se. No post deposition heat treatment is required.

A SEM cross-section of a CIGS film deposited at 12 inches/minute (30.48 cm/minute) is shown in Figure 3.6A, and can be compared to material deposited at the standard rate of 6-

inches/minute shown in Figure 3.6B. Morphology of the film appears to be excellent with a large, dense grain structure. In fact, the morphology of the film deposited at 12 inches/minute (30.48 cm/minute) appears to be better than films deposited for longer time intervals. The film thickness is approximately 1.8 μm .



Absorber deposition at such high rates is significant because deposition rate for the absorber is one of the rate limiting steps for module production. The absorber deposition is also capital intensive, so ultimate module cost as well as production throughput are improved with higher rate absorber deposition.

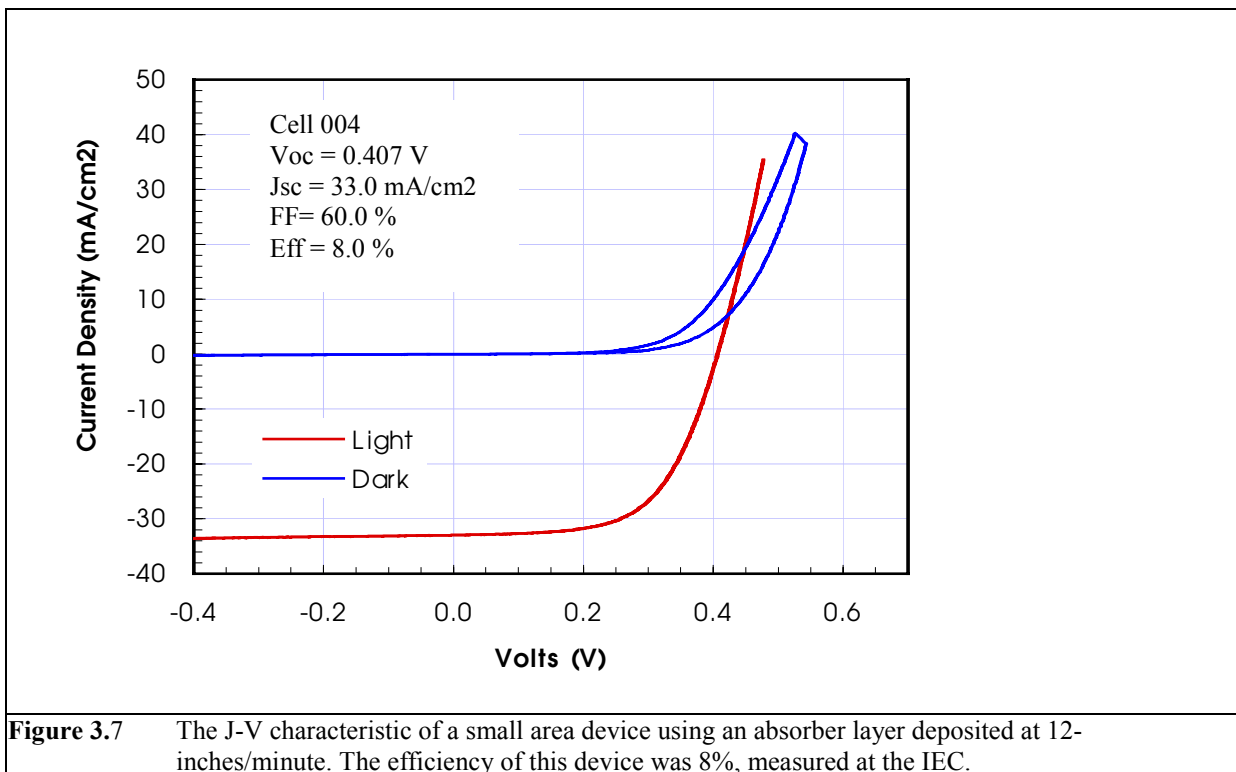
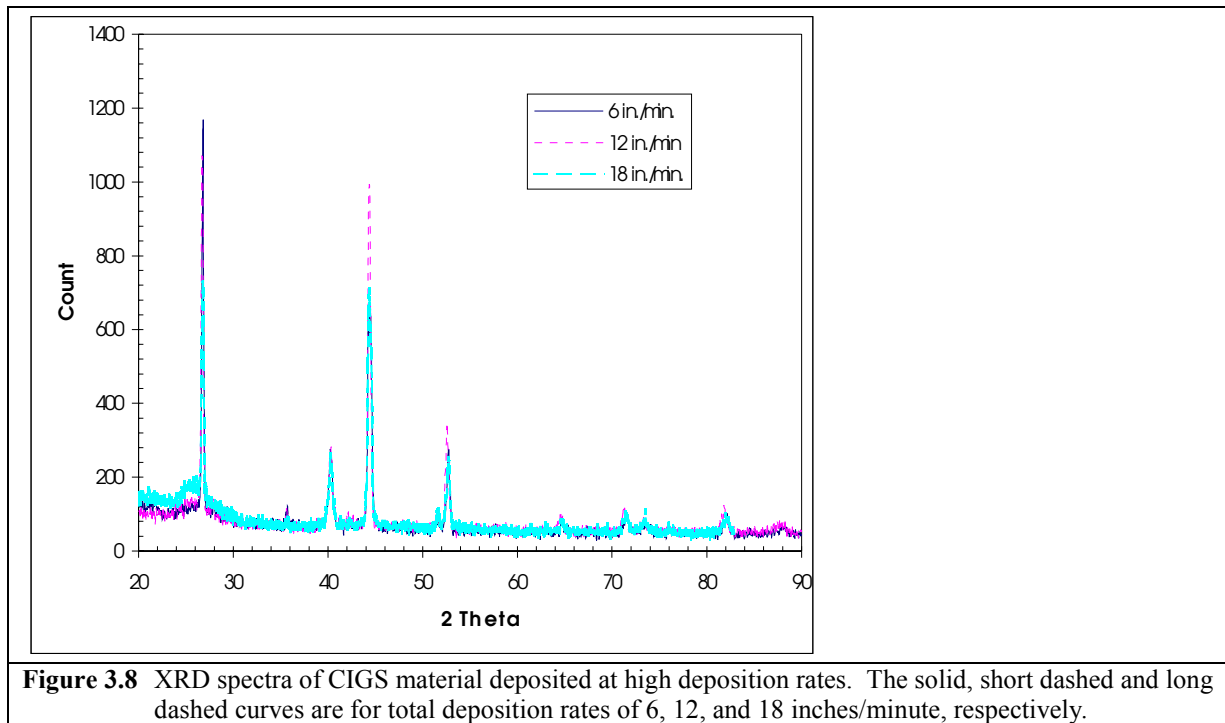


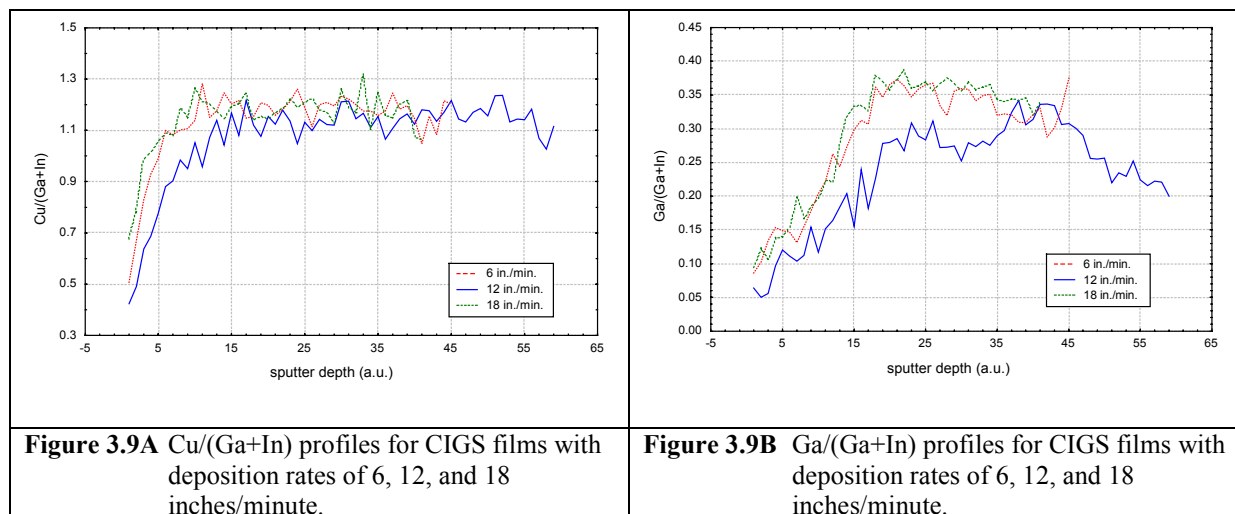
Figure 3.7 The J-V characteristic of a small area device using an absorber layer deposited at 12-inches/minute. The efficiency of this device was 8%, measured at the IEC.

There has always been uncertainty about the limiting minimum time in which high quality CIGS can be formed. Deposition times for high quality CIGS in a number of laboratories are typically 30 to 45 minutes. CIGS has been deposited with the metals flux delivered in as little as 5 to 12 minutes (but with extra selenization afterwards) in a laboratory setting. At 12 inches/minute within a small (proprietary) reaction zone, we believe that we have deposited CIGS at the fastest rate ever. Samples of this high rate CIGS were finished resulted in devices having 8% efficiency (J-V shown in Figure 3.7).

Utilizing the capability of the evaporative sources under development at GSE, we have deposited CIGS films (including Se exposure) **at web speeds of up to 24 inches/minute**. Absorber formation in such brief times might be expected to affect the polycrystalline material growth and film morphology. Additionally, composition gradients that occur as a result of the source sequence during the deposition may be expected to be affected given such short time in the high temperature Se-containing environment. However, the XRD data shown in figure 3.8 appears to indicate little difference in the crystalline orientation and phases formed at these high rates compared to the baseline rate of 6 inches/minute.



Critical ratios from Auger depth profiles have been measured on CIGS deposited rates of 6, 12, and 18 inches/minute (Figure 3.9A and 3.9B). There are no major qualitative differences in the elemental profiles between the films. Taken together with the x-ray data, the implication is that, for the approach taken at GSE, diffusion processes do not limit the formation rate of CIGS films.



CIGS films have been deposited at web speeds of up to 24 inches/minute, but only to a thickness of 1.0 μm . Rates as high or higher than this will require modifications to extend the capabilities of the effusion sources.

CIGS deposition at any of these high rates exceed the PVMaT end-of-contract goal (27 cm/minute) and is one of the major tasks for the planned 3 year program.

3.4.5 Impurity Incorporation in the CIGS

Higher-rate deposition of CIGS films generally entails higher effusion source temperatures. A potential source of concern is increased generation of impurities from the effusion sources (heat sources, insulation, etc.) and the support structure around the sources that become incorporated in the CIGS film. Any evidence of impurity incorporation needs to be determined early on so that data is not misinterpreted and the appropriate changes can be made to the CIGS deposition environment. Several of the high-deposition rate films have been submitted to NREL for SIMS analysis to investigate this potential problem.

Although the materials comprising the source insulation and in the immediate vicinity of the deposition zone were specially selected to withstand the high-temperature, selenizing environment, there was no direct confirmation that these materials were not decomposing and being incorporated into the CIGS film. Impurities can be deleterious if they are electrically active or affect crystallinity.

Three CIGS films deposited in total deposition times corresponding to web rates of 6, 12, and 18 inches/minute were submitted for SIMS depth profiling at NREL (S. Asher) to determine if high rate deposition had any significant effect on impurity incorporation. The CIGS films were of thickness 1.5 – 2.0 μm . The particular elements analyzed for were C, Na, Cl, Fe, Cr, O, and Si. The SIMS profiles for these samples are shown in Fig. 3.10. For the purposes of comparison, all signals are normalized to the Se signal.

There is virtually no difference between the films in the concentration of Fe and Na. The concentrations of O, C, Cl, Cr, and Si are actually slightly lower in the CIGS films deposited at 12 and 18-inches/minutes than in the film deposited in 6 inches/minute. The results imply that impurity concentrations are low and that there should be no strong concern regarding impurity incorporation at the higher deposition rates.

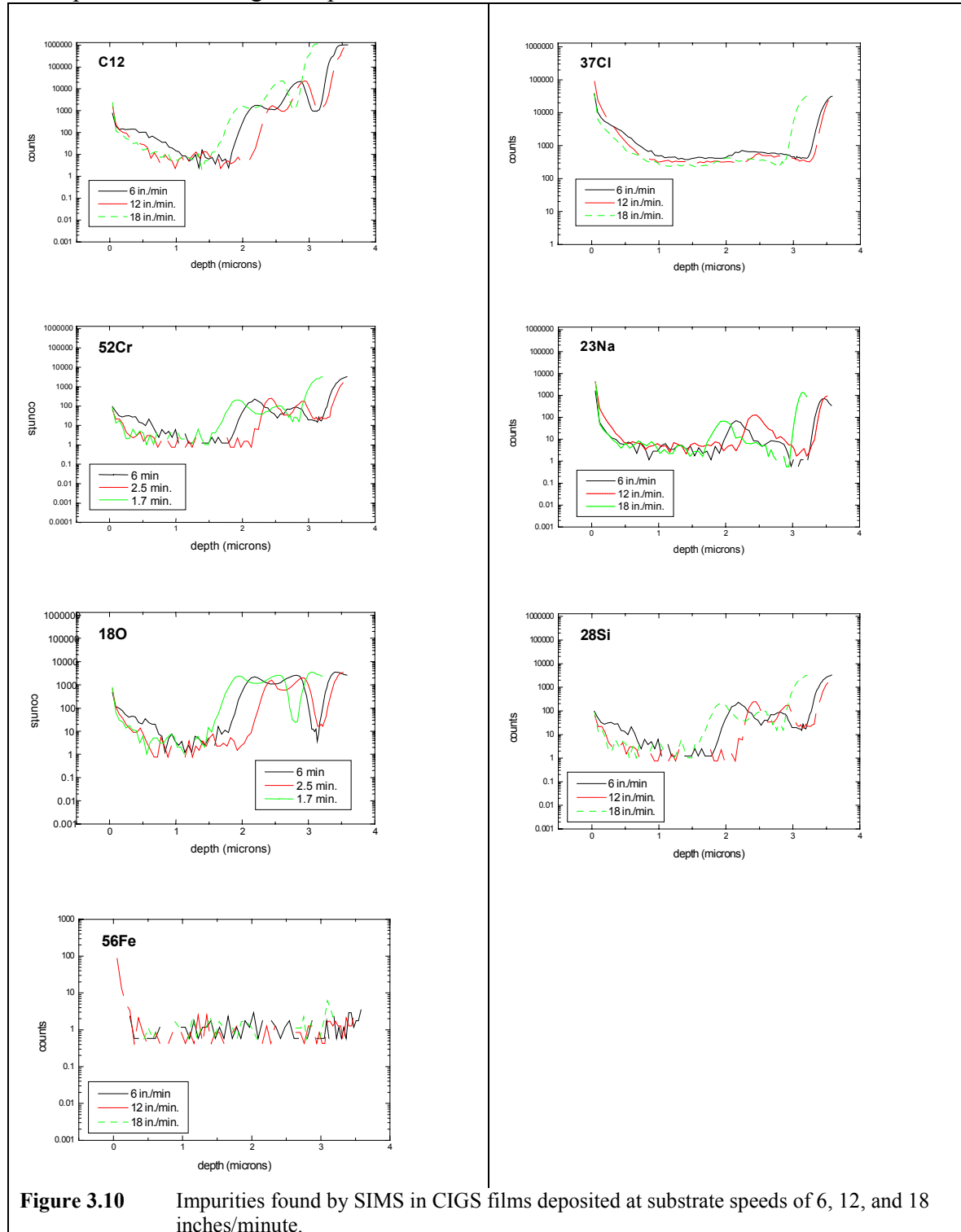


Figure 3.10 Impurities found by SIMS in CIGS films deposited at substrate speeds of 6, 12, and 18 inches/minute.

3.5 Conclusions and Future Work

At GSE we have been successful in developing methods for high rate deposition of high purity CIGS using a low temperature, roll-to-roll process on flexible polyimide substrates. CIGS deposited in continuous roll-to-roll process is of reasonable quality, as indicated by device results, even at substrate rates that exceed the PVMaT end-of-contract goal. The aspects of this task associated with the highest risks (scaled-up evaporative source design and very high rate CIGS formation) have already been attacked, with good result. Deposition of CIGS by co-evaporation at very high rates over large areas appears to be viable.

The design and use of effusion sources will undergo evolutionary modification to further improve CIGS uniformity, control, film composition and device efficiency. Although the adhesion of the CIGS has been acceptable under many conditions, more work is required to fully understand the factors involved, including interaction with the back contact. Systematic experiments must begin to determine the dominant causes affecting CIGS/back contact adhesion.

More work is required to extend the operational control and reliability of the CIGS deposition components, including the sources, to attain longer runs of roll-to-roll material. Work here will also likely involve means to thermally stabilize the deposition environment over longer periods of time.

4.0 Task 4: In-Situ Sensors for Intelligent Process Control of Roll-to-Roll CIGS

4.1 Introduction and Problem Statement

To assess the quality and heterogeneities of the final vapor deposited film and the individual processing steps, the conventional procedure is to conduct a post analysis of the completed device using measurements that are sensitive to structural and electronic properties. However, the fundamental mechanisms underlying processing and materials performance relationships in more complex and dynamic thin-film structures, may not be revealed in post-processing measurements. For these cases, effective feedback process control is critical and underscores the need for real-time measurement and interpretation of system parameters. This will require that an open architecture process control system be adopted that combines sensor data and results from physical based models with control algorithms.

Although process models and simulators enable development of effective process reactor designs and model-based control strategies, real-time sensing and control of critical process and product variables is required to accommodate unanticipated process upsets, reactor variability/drift, and perhaps allow operation in physically unstable processing regimes where repeatability can be achieved only through dynamic feedback/feedforward control. The future of advanced materials processing will involve active control of the fabrication and real-time monitoring of the composition and physical properties of the vapor before deposition and of the thin-films after deposition. This will enable active adjustment of the growth program to maintain the necessary development of the coating. Sensors must be an integral part of the overall material processing system. They must provide accurate information about the composition and physical condition of the material that is being deposited and the stoichiometry, microstructure, and electronic properties of the films as they are growing. These data must be acquired non-evasively and as rapidly as possible. This is a significant challenge that represents the frontiers of high-tech materials science.

Sensor evaluation and selection is based upon their suitability to provide accurate and reliable information to the process controller both on conditions within the CIGS deposition zone and on the characteristics of the film after it leaves the deposition zone. The primary controlled parameter is the power supplied to each of the effusion sources. The technique(s) must be adaptable to the design and manufacture of an inexpensive, versatile, and robust, in-line sensor that can provide *in situ* process control information in the harsh environment of a vapor deposition chamber where heat and coating of sensor components can damage or interfere with the instrument.

In the present CIGS deposition system, thermocouples provide information about the effusion source temperature and physical based models provide guidance about expected effusion flux and anticipated film properties. In general the effusion source temperature and effusion property measurements enable more direct and simple process control but are less closely tied to desired film properties whereas in-situ measurements of the samples provide information about film properties but require more sophisticated "intelligent" process control. While it may be

impractical to develop in-line sensing to measure all product variables of interest, the sensors must identify physical properties of the effusion and deposited films that are related to product performance and that can be used for process control.

4.2 Task Goals

Diagnostic development is necessary to enable real-time control during the absorber deposition for the extended times necessary to process up to 1000 feet of substrate. Cost and yield improvements will result from better control of the CIGS properties in the roll-to-roll process. Thus in-line or on-line sensors with appropriate sensitivity to key electronic and physical CIGS properties must be developed and implement in the deposition system. The sensor(s) must be robust, reliable, and suitable to in-situ deposition conditions. In addition, algorithms for data reduction must be developed to provide meaningful and predictive output for real-time operation and integration with existing control architecture.

The goal of this portion of the project is to develop equipment and methods for real-time, in-situ intelligent control that:

- Demonstrate sensitivity to, and is predictive of the crucial electrical and physical properties of the CIGS absorber material.
- Design and install practical equipment on laboratory scale reactors, and finally on production equipment.
- Develop a robust, practical algorithm to reduce raw data to information that is uniquely predictive of the important electronic and physical qualities of the CIGS.

4.3 Technical Approach, Equipment Capability – Spectroscopic Ellipsometry

It has been particularly useful to concentrate on the polarization state of light reflected from deposited films, and how this is modified through the interaction with the sample. A spectroscopic ellipsometer (SE) sensor that we are developing has the potential of measuring several thin-film properties simultaneously, such as thickness, composition, and resistivity; providing the real-time sensing required for effective CIGS process control. Unlike conventional ellipsometers, which measure the intensity of the reflected polychromatic light for each polarizer orientation, our SE utilizes carefully selected polarization states (intensities) to determine complex reflectance and/or ellipsometric amplitude (Ψ) and phase (Δ).

Even though our SE sensor has been shown to have a simple architecture, its true real-time processing capability is still dependent on the development of an efficient spectra-structure transformation algorithm(s) to handle the large dimensionality of the input parameter space/data set. In addition, with the advent of high-speed microcomputers and efficient end-point predictors (such as the neural networks), we intend to extract meaningful interpretations of ellipsometric data so as to be practically simultaneous with the measurement; i.e., a back propagation network

will be used to quickly interpret spectroscopic ellipsometric measurements in contrast to conventional analysis which uses a linear regression to fit parameters to a thin-film model.

Spectroscopic Ellipsometry (SE) -- By measuring the change in polarization state of reflecting light, the ellipsometer is an optical probe that is uniquely suited for in-situ analysis and control of growing films. It is nondestructive, measurements are acquired quickly with sensitivity to films less than a monolayer in thickness, and an ultrahigh vacuum is not required.

An ellipsometer is designed to measure changes in the relative amplitudes (Ψ) and phases (Δ) between the p and s electric field components of a monochromatic light beam (fully polarized light wave) as it reflects from the sample. These parameters are traditionally expressed as Ψ and Δ , which are related to the ratio (ρ) of the reflectance coefficients for the optical electric fields parallel (p) and perpendicular (s) to the plane of incidence.

$$\rho = \tan(\Psi) \exp(i\Delta)$$

The amplitude and phase change parameters (Ψ , Δ) obtained in ellipsometry can also be expressed in terms of the changes upon reflection in the angular orientation and ellipticity of the polarization ellipse associated with the incident wave. Unlike a reflectance measurement, which only provides the ratio of reflected to incidence irradiances, an ellipsometer can extract both real and imaginary parts of the dielectric function, (ϵ_1, ϵ_2) , as a function of the photon energy, $(h\nu)$, from the (Ψ, Δ) measurement.

As discussed above, the ellipsometer is a unique technique in that the real and imaginary parts of the dielectric function can be extracted directly as a function of photon energy. For the homogeneous, layer-by-layer growth of a perfectly uniform transparent or absorbing film on an ideal, fully characterized substrate, real-time ellipsometry at a single photon energy has been shown to provide the dielectric function of a film along with its thickness. The dielectric function, $\epsilon(\omega, K)$, which describes the response of a material to an electromagnetic field has significant consequences for the physical properties of a solid. It depends sensitively on the electronic band structure (and other physical properties) of a material and studies of the dielectric function by optical spectroscopy (multi-frequency response) are very useful in the determination of a material's overall band structure.

Several spectroscopic ellipsometry systems have been designed for in-situ process monitoring. Some can be purchased as an integrated device. However, there are no spectroscopic ellipsometers currently available (either commercially or in any reported development laboratory) that acquire all of the necessary information in a single, instantaneous sampling; nor are these systems cheap. Since no spectroscopic ellipsometer with appropriate capabilities is commercially available, we are developing a novel Spectroscopic Ellipsometer sensor for in-line, real-time control of CIGS manufacturing processes. The SE sensor we are developing has the potential of measuring several thin-film properties simultaneously, such as thickness, composition, and resistivity, and providing the real-time sensing required for effective CIGS process control (spectroscopic data can now be acquired in parallel over a wide photon energy range in less than 20 ms).

4.4 Results, Equipment Status

As an example of the type of data that our SE produces, Figure 4.1 shows spectra obtained with our initial bench top SE instrument. The data in Figure 4.1 were obtained from a flexible CIGS sample and represent “raw” spectral distributions of different polarization states that comprise the complete polarization information.

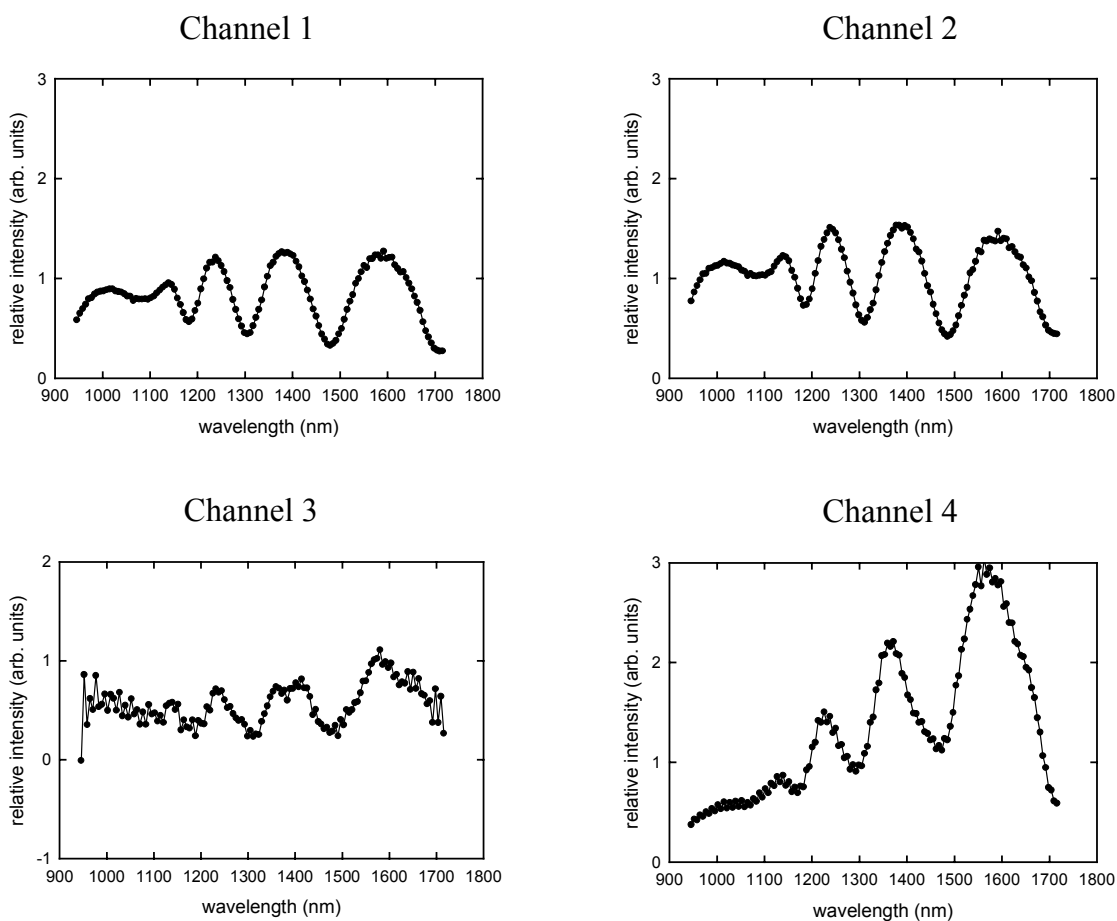


Figure 4.1. Raw SE Spectral Data Collected from Flexible CIGS films [Cu/(In + Ga) = 0.89]

Interference due to optical reflection at the interfaces between the semiconductor layers and the substrate cause the oscillations in the spectra (Figure 4.1). A complete analysis involves processing these data through the instrumentation matrix to extract the complex dielectric function and, from that, the material-dependent properties of the device.

The fabrication of flexible CIGS photovoltaics involves the deposition of a CIGS thin film onto a Mo film deposited on a flexible substrate. A model for this system that is used for analytical calculations is shown in Figure 4.2. To illustrate the capabilities of spectroscopic ellipsometry with CIGS samples, several samples were prepared and tested, a few blind (i.e., the composition was not provided). The samples were produced with different film thickness, film quality, and composition. The Cu/(In + Ga) composition ratio of four samples along with the Ga/(In + Ga) ratio of two of these samples were provided. Ellipsometry measurements were performed with six CIGS samples. The provided composition ratios along with the measured ellipsometry results are shown in Table 4.1. The ellipsometry results were obtained from a systematic analysis of the raw data that included extraction of the physical contributions. The measured composition ratios, CIGS film thickness, surface roughness and measured band gap results were determined for each of the samples and are tabulated in Table 4.1.

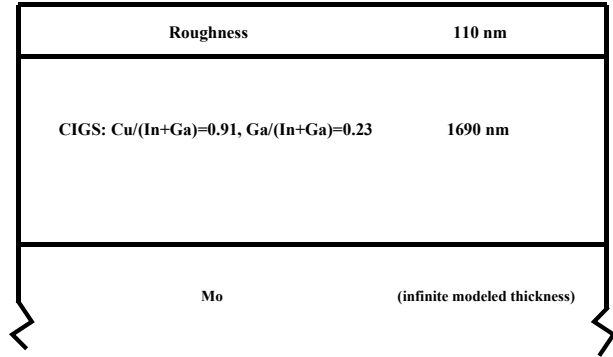


Figure 4.2. Model of CIGS Samples used for Calculations

Table 4.1. Measured Ellipsometer Results from CIGS Samples. The band gap was calculated with the equation $E_g = 1.0032 + 0.71369y$, with $y = \text{Ga}/(\text{In} + \text{Ga})$; except a356, where the following equation was used $E_g = 1.011 + 0.664y + 0.249y(y-1)$. (Note: + = 'good', o = 'moderate', - = 'poor')

Sample	Ga/(In+Ga)		Cu/(In+Ga)		Quality		Physical (nm)		Band Gap
	Optical	Given	Optical	Given	Optical	Given	Thickness	Roughness	
a306	0.29		0.77		o		3100	85	1.21
a336	0.24	0.15 - 0.25	0.69	0.88	+	+	1610	112	1.17
a343	0.25		0.77		+		2000	157	1.18
a356	0.26		0.96	1.14	-		1650	160	1.14
a358	0.24	0.20 - 0.40	0.91	0.91	+	+	1690	110	1.17
a375	0.19		0.59	0.67	o		3200	120	1.14

The optical properties not only contain a great deal of information about the nature of the sample but can also serve as an indicator of quality control. A spectrum consisting of the pair of tables $\Psi(l)$ and $\Delta(l)$ is sensitive to almost any physical or electronic property that would be of interest to a materials processor. However, in a sensing application it is not practical to perform a detailed analysis for all of the material properties of interest. Provided that a spectrum can be rapidly obtained, it is possible to design interpretation algorithms that automatically identify the features of interest. It is likely that the resulting information will involve interpretable parameters, including: the film

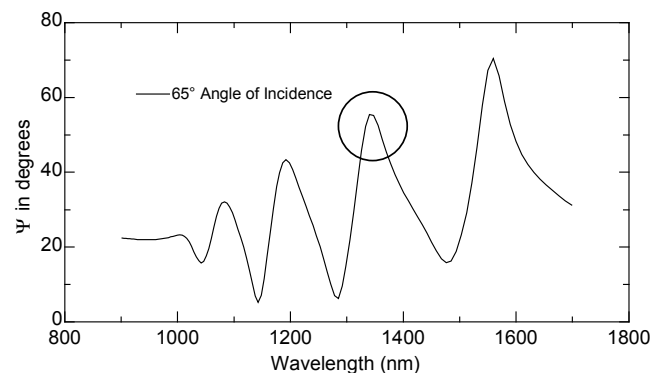


Figure 4.3. The CIGS Spectral Fingerprint will be used to Design Interpretive Algorithms that Automatically Identify the Features of Interest

thickness, surface roughness, optical bandgap, stoichiometry, grain boundary effects, stress, foreign phases, interface mixing and other material qualities. In addition, a spectral fingerprint (Figure 4.3) can be used as a “good sample” versus “bad sample” identifier. Such an approach requires the assembly of a catalog of reference data on samples grown under different conditions. Once obtained, the database can be used to provide a very practical evaluation of the processing that is being performed inside the deposition chamber, even if the detailed interpretation of the measurement is not available or desirable.

The spectral fingerprint approach was demonstrated with the CIGS samples. An ellipsometry spectrum of each CIGS sample was used along with interpretive algorithms to generate a quality factor (Figure 4.4). By comparing a specific quality factor from different samples, a criterion can be established to differentiate between “good” and “bad” samples. A comparison between quality factors for the CIGS samples is shown in Figure 4.5 and summarized in Table 4.1. The measured ellipsometry quality factor results are in good agreement with the GSE assessment of the samples (Table 4.1).

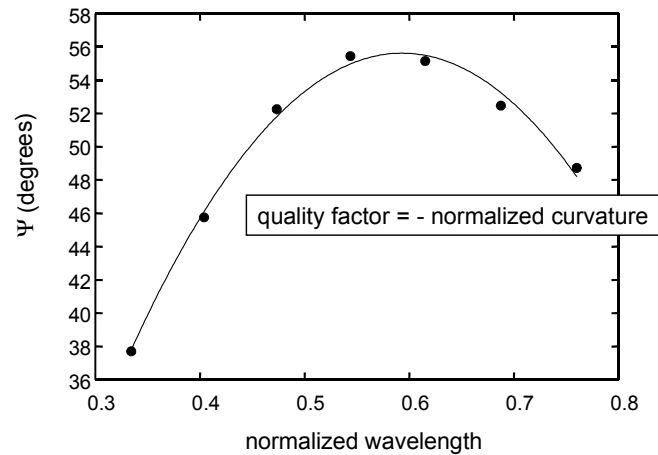


Figure 4.4. A Representative Plot used to Generate the Quality Factor for each CIGS sample

The previous demonstration shows how even a simple analysis of spectroscopic ellipsometry data can lead to valuable insight about a sample that could not be extracted with other sensor methods. Beyond this, however, since the ellipsometer is sensitive and reproducible, it is possible to identify “fingerprints” of “good” and “bad” material, even without a complete interpretation of the spectra. Because of this, spectroscopic ellipsometry can be installed in almost any thin-film fabrication operation as a real-time process monitor. However, high-speed operation that is much faster than is currently available with commercial systems would be required to achieve this goal.

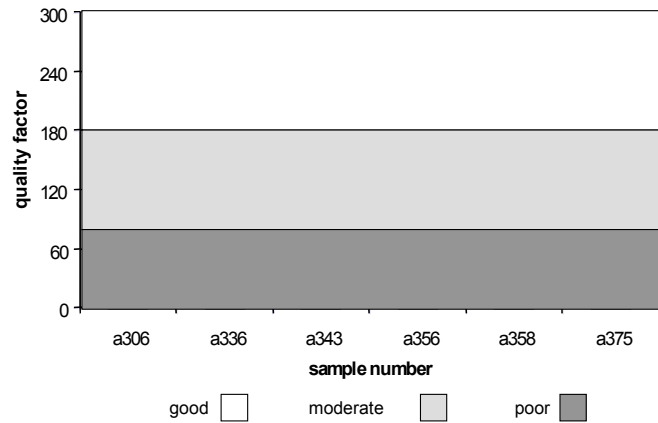


Figure 4.5. Application of the Quality Factors to CIGS Samples

4.5 Current Status, Conclusions

Our SE sensor is based on an original design crafted to overcome some of the intrinsic limitations of conventional ellipsometry instruments. The SE will provide reliable measurements of the CIGS films from a flexible moving support. The present development of our SE system is on schedule. The design and construction of the individual system components is complete. In addition, an auto-alignment system is being tested. A prototype instrument should be available for testing within two months. The testing will demonstrate the unique data collection capability of the instrument and the ability of the SE to provide reliable information about the CIGS film properties. An operational SE should be available by September 1999. The interpretive algorithm development and process control integration is also on schedule.

4.6 Future Work, Plans

The main issues yet to be resolved involves insertion of the SE into an actual deposition system, performing in-situ data collection, and the level of interpretive algorithms that will be used. Initially, a conventional interpretive algorithm will be developed, based on effective medium theory and heuristic learning and regression, to determine specific properties of interest. This may simply involve “spectral finger print” type analysis or more sophisticated models based on measured optical parameters. Ultimately, a next generation, 'smart' interpretive algorithm(s), may be developed and applied to the CIGS processes, but this will require a significant increase in the present research and development effort for our SE. In either case, both approaches will need to be validated in the CIGS deposition process.

Transformation Algorithms Based on Heuristic Techniques - The relationship between the complex spectrum and meaningful material parameters is achieved by means of a mathematical model. For example, the three-phase system consisting of a substrate, a surface film, and air can be handled by standard electromagnetic boundary conditions. If the substrate characteristics are known, then the meaningful material-dependent information about the film may be its thickness, surface roughness, void fraction, and density of some particular electronic defect. By knowing how each of these characteristics influences the optical properties of the film, one can use the model to calculate the experimental complex ρ spectrum. The usual way this is accomplished is by means of conventional multi-parameter linear regression, which can take considerable time (Figure 4.6).

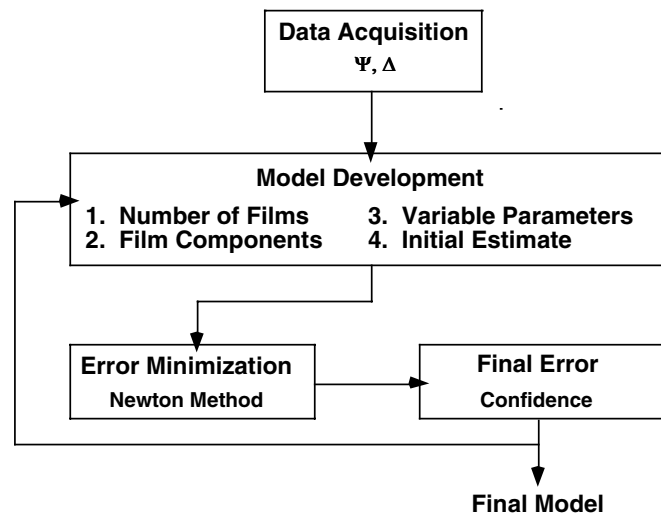


Figure 4.6. Conventional inverse parameter fitting method for determining properties

In this context, data acquisition and analysis may be 20 seconds. This is totally unacceptable for a true-real-time sensor instrument.

Our approach is to perform heuristic *training* of transformation algorithms (eg. limited regression based on spectral finger print identification or a neural network) to handle input spectra and directly generate the desired output. Each element of information (or *neuron*) exists in one of several *layers*. One layer is the input spectrum. The last layer is the set of desired parameters. Connecting these are one or more *hidden layers*. Each neuron beyond the input layer receives weighted information from each of the neurons in the earlier layer. It also contributes, by suitable weights, to each neuron in the next layer. A properly trained network has had its weights adjusted so that, for a given input configuration, the output layer adopts values that are very close to correct. With a quick application of a conventional fit, the exact values for the parameters in the output layer can then be determined.

A complex network can be trained in a few hours. However, once trained, it will efficiently process input spectra so as to provide meaningful output. The intermediate step of extracting various forms of spectrally resolved data is completely eliminated; thin-film property measurements are extracted in essentially real-time.

Construction of Smart Algorithms - At present, real-time control of the film growth processes with “raw” polarization state data is ad-hoc, requiring pre-trained, pre-calibrated correlations to key electronic properties of the film. In this case, “pre-training” methods are unsupervised without taking into account (and/or learning from) the subtle variations in film properties which occur during the processing. Proposals have been submitted to develop and implement an approach based on the supervised learning methods used in acoustic signal and imaging processing. With these methods, we will be able to develop an algorithm(s) that will automatically extract key features of the ellipsometric spectra and then use these features (basis) to predict physical properties of the film.

5.0 Alternative Back Contacts

5.1 Task 5 Introduction

Molybdenum (Mo) has been used almost exclusively as a back contact material for CIGS-based photovoltaics. Key beneficial features of Mo include: high electrical conductivity, ohmic contact to CIGS, and high temperature stability in the presence of selenium during CIGS absorber deposition. Nevertheless, GSE has identified a few issues regarding Mo. Mo is an expensive brittle material that exhibits large intrinsic stresses when deposited by sputtering. The compressive stress in the Mo complicates substrate handling and transport, as it has a tendency to curl or roll up even when constrained under tension between rollers. Intrinsic film stresses can be controlled by choice of sputter deposition working gas pressure, however, Mo deposited at higher pressures exhibited other problems.

Additionally, sputtered Mo does not adhere well to the stainless steel chamber walls resulting in excessive Mo debris generation. As a result, Mo production chambers require frequent cleaning to remove debris.

Problems with Mo as the back contact material also extend to glass substrates. When deposited at low sputter working gas pressures (achieving dense, near bulk electrical resistivity), adhesion to glass is poor, whereas at high sputter pressures adhesion is good but at the expense of increased resistivity. High pressure/low pressure bi-layer Mo is often used but transition to in-line automated manufacturing will require two chambers to deposit the back contact layer, thereby increasing cost.

Goals for GSE entail large-scale production of thin film CIGS for all market segments: utility, consumer, and space. In meeting these markets, the cost of every manufacturing operation in the production of CIGS modules must be considered. Deposition of Mo as the back contact is currently a significant issue with regard to meeting our ultimate cost goal. Mo as the back contact impacts cost by: the cost of raw materials, delivery time (cost of working capital), down time for chamber cleaning, and reduced yield from Mo particulate on the substrate caused by poor adhesion Mo to stainless steel vacuum chamber walls.

5.2 Task Objectives

GSE is investigating alternative back contact materials that can be engineered to avoid the difficulties associated with Mo. Lower melting point materials should be less prone to stress retention. Candidate materials must also be low cost and must be tested for compatibility with CIGS device stack formation and module processing.

Under the PV-MaT program, GSE is investigating alternative back contact materials. Results from this task should be applicable to other substrate including glass, polymer, and metal foil.

Quantitative benefits expected from the back contact task under the PVMaT program include:

- Reduce cost of back contact deposition operation by 50%,
- Reduce raw material cost by 50%,
- Reduce scheduled and unscheduled downtime by 50% by reducing particulate contamination, and
- Increase step yield to 99% by eliminating frequent arcs or shunts from Mo debris.

Cost modeling indicated that the above items correspond to a reduction in cost and an increase in capacity by achieving a reduction in direct materials cost, operating cost, and downtime while improving yield.

5.3 Technical Approach

Technical approach for the alternative back contact task involved investigating different metals and alloys as well as bi-layers. Bi-layer configurations consisted of Mo in direct contact with CIGS and an underlying layer that provides the bulk of the back contact sheet resistance and controls the stress state.

Initially candidate back contact were identified by a review of past literature and by discussions with organizations involved with CIGS development. With candidates identified, both single element and bi-layer materials were analyzed for potential reaction with primarily selenium. Single element back contacts were deposited at IEC and sheet resistance and crystallography were characterized. CIGS was deposited on the most promising single component back contacts and finished to devices to measure the ohmic behavior of the interface.

In parallel, bi-layers were deposited in GSE roll-to-roll production-based equipment. Two promising bi-layers that consist of a conductive underlying layer and Mo as the overlying layer were deposited. Back contact uniformity was characterized by measuring across-web and down-web sheet resistance. CIGS was deposited on candidate bi-layers in GSE roll-to-roll production-based equipment and devices were characterized to assess behavior of the back contact.

5.4 Results

5.4.1 Background and Candidate Material Identification

The back contact base layer in a CIGS module serves to collect photogenerated current. Desirable film characteristics and deposition properties for the back contact include:

- Good bonding to the substrate,
- Sheet resistance of less than 1 ohm/sq., analysis indicated less than a 1% power loss due to series resistance for a CIGS module with a cell spacing of 0.5 to 0.75 cm at AM 1.5,
- Amenable with high rate deposition,
- Low cost, readily available raw material,

- Stability at CIGS processing temperatures of 450°C to 600°C in selenizing environment, and
- Neutral or slightly compressive stress.

Metal contacts with CIS were investigated by NREL in the early 1980s [Ref 5-1]. Candidate back contacts included platinum (Pt), gold (Au), silver (Ag), nickel (Ni), copper (Cu), aluminum (Al), and molybdenum (Mo). According to these early NREL studies (as summarized in Table 5.1), Au and Ni were the best and most reproducible contacts to CIS with clean interfaces and no evidence of reaction. Good ohmic contact was also achieved with Ag, but Ag had a tendency to diffuse in CIS and dope it to n-type. Al was generally a good ohmic contact but was unstable due to natural oxide formation and could not withstand CIS processing temperatures. Mo was reported to exhibit a slight diode behavior but had a low contact resistance to CIS and was stable with no detectable reaction.

Despite the positive results with Au and Ni, both were eliminated as serious candidates for the back contact to CIS. Au is expensive and limits the ultimate PV cost whereas Ni was difficult to sputter at a high rate. As a result, Mo became the leading candidate for the back contact and is the material most widely used by researchers and industry. Key attributes of Mo include: low sheet resistance, low contact resistance, stability at CIS deposition temperatures, amenable to high rate deposition processes such as sputtering, reasonable cost compared to Pt, Au and Ag, and phase stability in contact with CIS, Cu, In, and Se.

Table 5.1. Ohmic behavior of CIS/metal contacts from NREL Work [Ref 5-1].

Metal	Configuration	Deposition Technique	Behavior	Reproducibility
Au	Substrate* On CIS†	Thermal Heating Thermal Heating	Ohmic Ohmic	Very Good Very Good
Mo	Substrate* On CIS†	d.c. Magnetron r.f. Magnetron d.c. Magnetron	Non-Ohmic Generally Ohmic Generally Ohmic	Good Very Poor Poor
Ni	On CIS†	d.c. Magnetron	Ohmic	Very Good
Al	On CIS†	Electron Beam d.c. Magnetron	Generally Ohmic Ohmic	Poor Good
Ag	On CIS†	Thermal Heating d.c. Magnetron	Generally Ohmic Generally Ohmic	Poor Poor
Cu	On CIS†	Electron Beam	Non-Ohmic	Poor (Degraded with time)

* CIS deposited onto metal, † Metal deposited onto CIS

Under the PVMaT program, GSE proposed and in-depth study on alternative CIGS solar cell back contact materials for both flexible and glass substrates. Initial candidate back contact materials included, but was not limited, to niobium (Nb), titanium (Ti), a nickel (Ni), and chromium. Additionally, layered structures consisting of copper, for example, to achieve low sheet resistance and a barrier layer to prevent reaction of copper with selenium were also investigated. GSE's unique monolithic integration approach allows consideration of bi-layers with copper as part of the back contact because the copper is never directly exposed to Se even after the back contact through-scribe operation.

Bulk properties of the several candidate back contact materials are listed in Table 5.2. In addition to the materials listed in Table 5.2, bi-layers and binary compounds such as nickel aluminides, titanium aluminides, nickel titanium, as well as conductive carbides and nitrides were investigated

Table 5.2. Key material properties and cost estimates for alternative back contact materials proposed for an in-depth investigation under the GSE PVMaT program.

Material	Electrical Resistivity, $\mu\text{ohm}\cdot\text{cm}$	Melting Point, $^{\circ}\text{C}$	Density gm/cm^3	Weight ft^2 of module grams	Cost of Target, $\$/\text{kg}$	Cost per ft^2 of module, $\$/\text{ft}^2$
Mo	5.2	2610	10.2	0.95	240	1.14
Nb	12.5	2468	8.57	0.80	149	0.60
Ni	6.8	1455	8.90	0.83	150	0.62
Ti	42	1660	4.5	0.42	52	0.11
Cr	12.9	1857	7.2	0.67	150	0.50
	~2.0	1083	8.92	0.83	50	0.21

† Accounts for Sputter Yield of 20%.

5.4.2 Single Layer Back Contacts -

5.4.2.1 Thermodynamic Analysis -- Thermodynamic analysis was conducted to assess relative stability of the candidate back contact materials in the reactive Se deposition environment. Reaction with Se was identified as the key degradation mechanism. Reactions that form intermetallics with In, Ga, and Cu, as well as reactions involving surface oxides, (i.e., TiO_x and Cr_xO_y) were ignored. Gibbs free energy of formation for several candidate back contact materials, including Mo, are listed in Table 5.3. Availability of data limited calculation of Gibbs free energy to Cr, Mo, Ni, Re, and Ti. Additionally, the reaction analysis does not account for kinetics and as a result even though a reaction is possible, formation may not occur at the GSE CIGS deposition temperature and time. Reaction analysis indicated all the alternative back contacts have the potential to react with Se. Most exhibited a ΔG of reaction that was greater than for Se/Mo reaction.

Table 5.3. Key physical properties and Gibbs Free Energy Calculation for Reaction with Se at 400°C .

Element	Electrical Resistivity [$\mu\Omega\cdot\text{cm}$] @ 20°C	Coefficient of Linear Thermal Expansion $\times 1e6$ [1/K]	ΔG (Metal/Se) [$\text{kcal}\cdot\text{mol}^{-1}$]
Cr	12.9	4.9	-80.00*
Mo	5.7	4.8	-40.31
Nb	15	7.3	**
Ni	6.84	13.4	-31.71
Re	19.3	6.2	-96.60*
Ta	12.45	6.3	**
Ti	42	8.6	-92.53*

5.4.2.2 Back Contact Deposition -- Back contacts of Ni, Cr, Ta, Ti, and Nb were deposited on glass substrates at IEC by e-beam evaporation. Although Re exhibited the lowest Gibbs free

energy for reaction with Se, films of Re were not deposited because Re is too expensive to be an economically viable back contact.

Each back contact was deposited on sodium lime silicate glass to achieve a target thickness of 2000 angstroms. Characteristics of each candidate back contact is listed in Table 5.4. Sheet resistances of Cr, Nb, and Ta were higher than expected and further examination of Cr, Nb, and Ta by X-ray diffraction indicated these films were amorphous. Ta was very difficult to e-beam evaporate due to the high melting temperature and compatibility with the e-beam crucible. Ta is also more expensive than the other candidate back contact materials and as a result would only be investigated further if it exhibited excellent ohmic contact with CIGS. The key reason for selecting Ta was as possible a reaction barrier between CIGS and a conductive base layer such as Cu in a bi-layer back contact configuration.

Table 5.4. Results of Alternative Back Contact Deposited on SLS glass.

Metal	1.1 Thickness [Å]	R _s [ohm.sq]	R [ohm.cm]	R _{bulk} [ohm.cm]	2. Observations
Cr	2000	4.5	90	12.9	RX: amorphous
Nb	2000	16	320	15.2	RX: amorphous
Ni	2000	0.7	14	6.84	flake off the soda lime
Ta	2000	24.6	492	12.45	deposition very hard. RX: amorphous
Ti	2000	4.5	90	42	Oxidation of the surface
Mo	10000	0.2	20	5.7	

5.4.2.3 CIGS Deposition -- CIGS was deposited on all alternative back contacts at IEC during a single run along with Mo back contact witness slides. Substrate temperature during deposition was limited to 400 °C to be compatible with GSE’s baseline flexible polymer substrate.

EDS composition analysis was conducted at 10 and 20 kV acceleration voltages after CIGS deposition. Results of the EDS analysis (Table 5.5) are listed as stoichiometry in terms of Cu/(In +Ga) ratios. Gallium concentrations were on the order of 7.5 to 9% resulting in calculated band gaps of 1.16 to 1.2 eV. No back contact elemental signals were observed on low EDS acceleration voltage composition profiles indicating that no apparent bulk diffusion of the back contact into the CIGS had occurred.

Table 5.5. EDS composition Results for CIGS Deposited on Alternate Back Contacts.

Sample	Back Contact	EDS (atomic %)					Cu [In+Ga]	Ga [In+Ga]	Eg eV
		Cu %	In %	Ga %	Se %	Sum %			
33014-11	Mo	21.70	19.03	8.84	50.43	100.00	0.78	0.32	1.19
33014-12	Ti	21.58	18.75	8.90	50.77	100.00	0.78	0.32	1.20
33014-13	Mo	21.40	18.33	9.75	50.52	100.00	0.76	0.35	1.21
33014-21	Mo	23.31	18.55	8.90	49.24	100.00	0.85	0.32	1.20
33014-22	Mo	22.98	17.97	9.29	49.76	100.00	0.84	0.34	1.21
33014-23	Ta	17.67	19.68	10.21	52.44	100.00	0.59	0.34	1.21
33014-32	Cr	21.37	18.92	8.78	50.93	100.00	0.77	0.32	1.19
33014-33	Mo	23.26	18.74	9.07	48.93	100.00	0.84	0.33	1.20
33016-22	Nb	19.76	20.93	7.40	51.91	100.00	0.70	0.26	1.16
33016-23	Nb	19.24	21.08	8.48	51.20	100.00	0.65	0.29	1.17

Devices were prepared on the CIGS samples using IEC “standard” solution grown CdS, i-ZnO, and ZnO:Al. Table 5.6 and Figure 5.1 summarizes the results of device testing for alternative back contacts as well as Mo witness specimens. Of the alternative back contacts, Cr appeared to be best, but was not as good as the baseline Mo. As compared to Mo, the Cr back contact exhibited a similar open circuit voltage but there was a reduction in Jsc and fill factor. The I-V curve for the Cr back contact showed both an increase in series resistance and decrease in shunt resistance. However no forward bias roll over was observed which may be attributed to formation of interface phases. Nb, Ti and Ta all exhibited poor cells eliminating these materials as direct ohmic contact to CIGS.

Table 5.6. Summary of Device Results for CIGS devices deposited on Alternative Back Contacts.

Sample	Metal	Voc	Jsc	FF	rEff	Roc	Gsc	Jmp	Vmp
		[V]	[mA/cm ²]	[%]	[mW/cm ²]	[Ω cm ²]	[mS/cm ²]	[mA/cm ²]	[V]
33014.32	Cr	0.5230	26.57	52.2	7.25	4.83	7	20.19	0.3591
33016.23	Nb	0.4983	25.71	38.3	4.90	14.23	6	18.56	0.2642
33014.23	Ta	0.5204	14.94	18.8	1.46	83.82	39	7.08	0.2061
33014.12	Ti	0.4031	22.13	31.7	2.82	15.84	25	13.25	0.2132
33014.21	Mo	0.5376	34.08	63.3	11.60	2.27	3	28.06	0.4134
33014.13	Mo	0.5478	31.32	63.0	10.80	2.58	2	26.04	0.4147

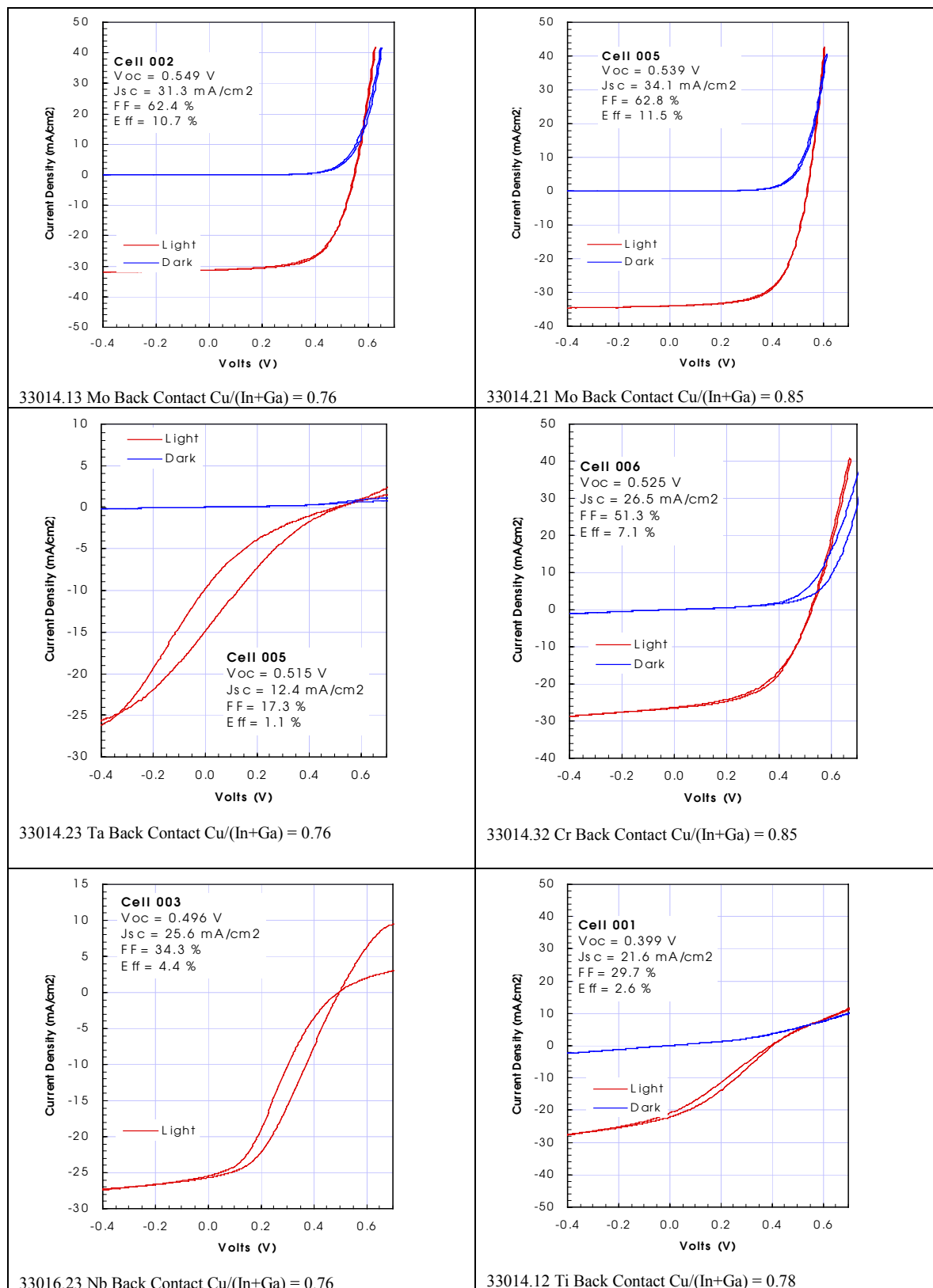


Figure 5.1. Representative I-V Curves for CIGS deposited at 400 C on Alternate Back Contact Materials

5.4.2.4 Large Area Deposition -- In parallel to the small area back contact work conducted at IEC, alternate single element back contacts were deposited using large area roll-to-roll deposition equipment. Deposition parameters were optimized to achieve sheet resistance values of 1 ohm/sq. at baseline production substrate speeds.

Of the back contacts, the more refractory body center cubic metals sputtered similar to Mo. Each exhibited high compressive stresses when deposited at low pressures and a stress crossover point at higher pressures.

Conversely, metals such as Cu and Ti exhibited much less stress, characterized by curling of the polymeric substrate. Resultant back contacts deposited on thin polymer substrates lie flat in an unconstrained condition. Additionally, these metals adhered much better to the stainless steel sputter chamber walls, significantly reducing debris even during processing of several thousand feet of substrate.

5.4.3 Bi-layer Alternate Back Contact -

5.4.3.1 Bi-layer Back Contact Deposition -- In addition to the single layer back contacts, bi-layers consisting of high conductivity base layers with overlying Mo were investigated. A key goal for the bi-layers were to reduce the Mo consumption by having the underlying layer be the major contributing layer to achieve a low sheet resistance and the overlying Mo layer provide good ohmic contact to CIGS. Bi-layer base materials were similar to those presented in Table 5.1 but also included additional materials such as copper.

All bi-layer investigations were conducted in existing GSE production-based equipment operated in a continuous roll-to-roll fashion. Preliminary investigations were conducted to optimize the layer thicknesses to achieve a GSE baseline sheet resistance values. During the Phase 1 effort, two key bi-layers were investigated.

Bi-layers back contacts were deposited on both 6-in. wide and 13-in. wide by 50 to 100-ft long rolls of polymer substrate. During initial studies, the deposition system was configured so an abrupt interface was achieved between the underlying conductive layer and the overlying Mo layer. A few deposition trials have been conducted with a graded interface between the layers but these films have not been characterized.

Figure 5.2 shows down-web uniformity of the bi-layer sheet resistance of one bi-layer configuration. Sheet resistance remained constant and within production control limits.

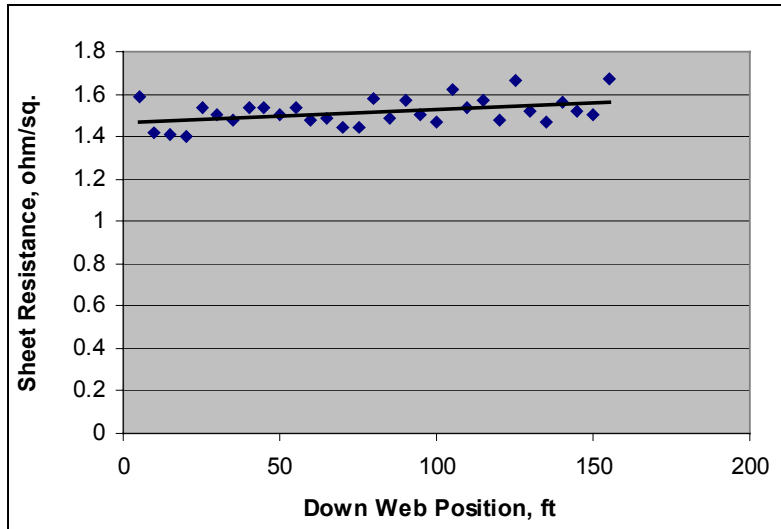


Figure 5.2. Sheet Resistance as a function of distance a bi-layer back contact for a 150-ft roll-to-roll deposition trial.

5.4.3.2 CIGS Deposition on Bi-layer Back Contacts -- CIGS has been deposited on two promising bi-layers that have Mo as the overlying layer in contact with CIGS. Resultant CIGS was adherent and passed routine tape tests. In addition there was no evidence of fracture of the back contact layer. However, one bi-layer exhibited severe stress after CIGS deposition and SIMs depth profiles indicated that the bi-layer base layer had reacted with Mo. For the other bi-layer, CIGS was successfully deposited. No increase in stress state was observed. SIMs depth profiles (Figure 5.3) indicated no reaction had occurred between the bi-layer constituents or with the CIGS elements.

Several devices have been fabricated on the bi-layer back contact including CIGS deposited at high rates under the PV-MaT program. IV measurement (Figure 5.4) revealed good ohmic contact with no evidence of forward bias roll over that may indicate reaction between the back contact and CIGS.

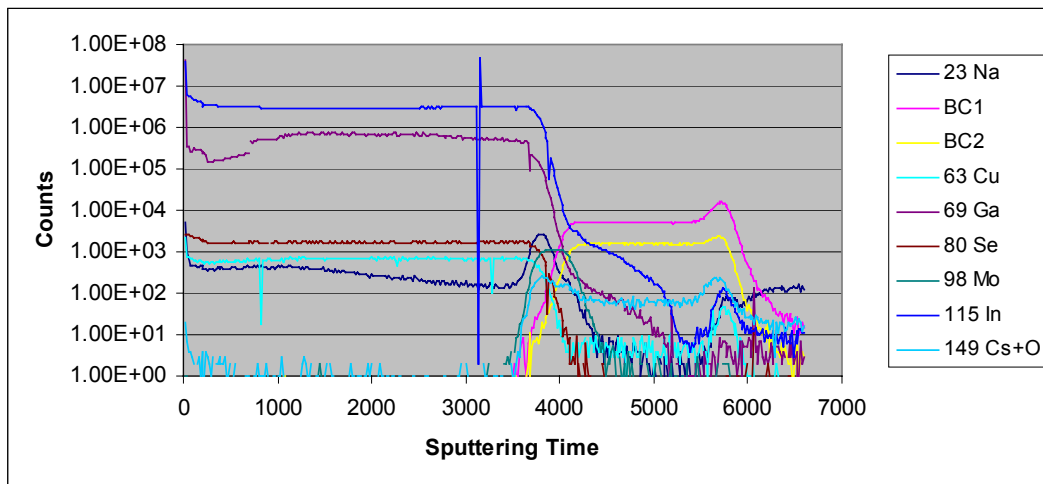


Figure 5.3. SIMS Depth profile for CIGS deposited on a bi-layer back contact showing no interdiffusion between layers.

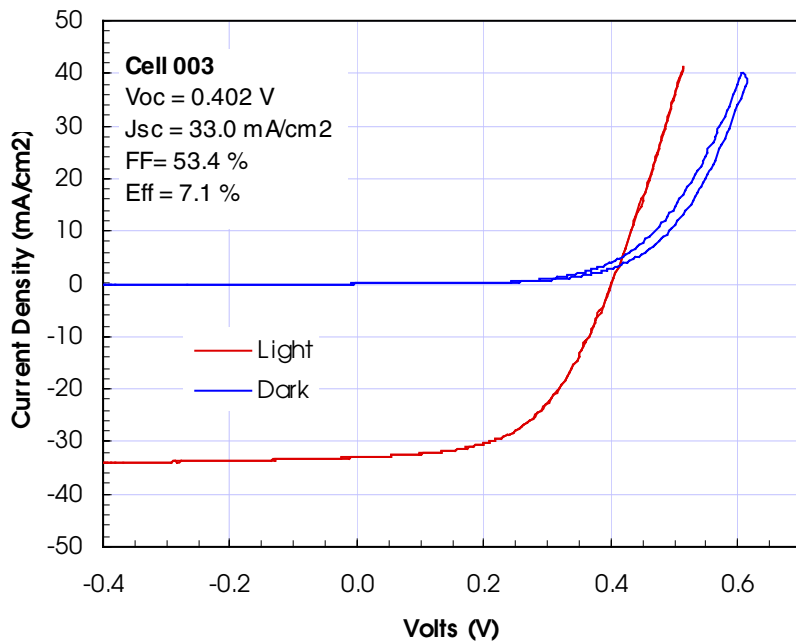


Figure 5.4. J-V for GSE Flexible CIGS Deposited on the Bi-layer Back Contact. The Figure Reveals an Ohmic Contact With CIGS.

5.5 Conclusions and Future Work

Currently one of the bi-layers has been baselined by GSE for flexible CIGS on polymeric substrates. Resultant back contacts meet sheet resistance goals and exhibit much less intrinsic stress than Mo. CIGS has been deposited and resultant devices are comparable in performance to pure Mo back contacts. Debris in the chamber has been substantially reduced allowing longer roll length between system cleaning.

Future work will concentrate on two key areas:

1. Optimizing the bi-layer that has shown good promise to replace straight Mo. Optimization will include using lower quality Mo as the overlying layer to reduce cost. Currently GSE uses expensive Mo that is twice as costly as lower quality Mo. Additionally GSE will quantify downtime associated with debris clean-up for comparing bi-layer back contact to straight Mo.
2. Secondly, GSE will continue to investigate candidate alternative back contacts focussing on bi-layers and tri-layers to further meet PV-MaT goals of reduced cost, improved yield, and decreased downtime.

REPORT DOCUMENTATION PAGE			Form Approved OMB NO. 0704-0188	
Public reporting burden for this collection of information is estimated to average 1 hour per response, including the time for reviewing instructions, searching existing data sources, gathering and maintaining the data needed, and completing and reviewing the collection of information. Send comments regarding this burden estimate or any other aspect of this collection of information, including suggestions for reducing this burden, to Washington Headquarters Services, Directorate for Information Operations and Reports, 1215 Jefferson Davis Highway, Suite 1204, Arlington, VA 22202-4302, and to the Office of Management and Budget, Paperwork Reduction Project (0704-0188), Washington, DC 20503.				
1. AGENCY USE ONLY (Leave blank)	2. REPORT DATE February 2000	3. REPORT TYPE AND DATES COVERED Phase I Subcontract Report, July 1998–July 1999		
4. TITLE AND SUBTITLE Photovoltaic Manufacturing Cost and Throughput Improvements for Thin-Film CIGS-Based Modules; Phase I Technical Report, July 1998–July 1999			5. FUNDING NUMBERS C: ZAX-8-17647-11 TA: PV006101	
6. AUTHOR(S) S. Wiedeman and R.G. Wendt				
7. PERFORMING ORGANIZATION NAME(S) AND ADDRESS(ES) Global Solar Energy, L.L.C. 5575 So. Houghton Rd. Tucson, AZ 85747			8. PERFORMING ORGANIZATION REPORT NUMBER	
9. SPONSORING/MONITORING AGENCY NAME(S) AND ADDRESS(ES) National Renewable Energy Laboratory 1617 Cole Blvd. Golden, CO 80401-3393			10. SPONSORING/MONITORING AGENCY REPORT NUMBER SR-520-27590	
11. SUPPLEMENTARY NOTES NREL Technical Monitor: R.L. Mitchell				
12a. DISTRIBUTION/AVAILABILITY STATEMENT National Technical Information Service U.S. Department of Commerce 5285 Port Royal Road Springfield, VA 22161			12b. DISTRIBUTION CODE	
13. ABSTRACT (Maximum 200 words) The primary objectives of the Global Solar Energy (GSE) Photovoltaic Manufacturing Technology (PVMaT) subcontract are directed toward reducing cost and expanding the production rate of thin-film CuInGaSe ₂ (CIGS)-based PV modules on flexible substrates. Improvements will be implemented in monolithic integration, CIGS deposition, contact deposition, and in-situ CIGS control and monitoring. In Phase I, GSE has successfully attacked many of the highest risk aspects of each task. All-laser, selective scribing processes for CIGS have been developed, and many end-of-contract goals for scribing speed have been exceeded in the first year. High-speed ink-jet deposition of insulating material in the scribes now appears to be a viable technique, again exceeding some end-of-contract goals in the first year. Absorber deposition of CIGS was reduced corresponding to throughput speeds of up to 24-in./min, also exceeding an end-of-contract goal. Alternate back-contact materials have been identified that show potential as candidates for replacement of higher-cost molybdenum, and a novel, real-time monitoring technique (parallel-detector spectroscopic ellipsometry) has shown remarkable sensitivity to relevant properties of the CIGS absorber layer for use as a diagnostic tool. Currently, one of the bilayers has been baselined by GSE for flexible CIGS on polymeric substrates. Resultant back-contacts meet sheet-resistance goals and exhibit much less intrinsic stress than Mo. CIGS has been deposited, and resultant devices are comparable in performance to pure Mo back-contacts. Debris in the chamber has been substantially reduced, allowing longer roll-length between system cleaning.				
14. SUBJECT TERMS photovoltaics ; Photovoltaic Manufacturing Technology ; PVMaT ; laser scribing processes ; ink-jet technology ; insulator deposition ; CuInGaSe ₂ ; CIGS ; high-rate CIGS deposition ; process control ; roll-to-roll CIGS; thin films			15. NUMBER OF PAGES	
			16. PRICE CODE	
17. SECURITY CLASSIFICATION OF REPORT Unclassified	18. SECURITY CLASSIFICATION OF THIS PAGE Unclassified	19. SECURITY CLASSIFICATION OF ABSTRACT Unclassified	20. LIMITATION OF ABSTRACT UL	